AD-A094 242 SAN FERNANDO LABS PACOIMA CALIF F/G 13/8
INVESTIGATION OF CNTD MECHANISM AND ITS EFFECT ON MICROSTRUCTUR--ETC(U)
OCT 80 D G BHAT N00019-78-C-0557
UNCLASSIFIED NL

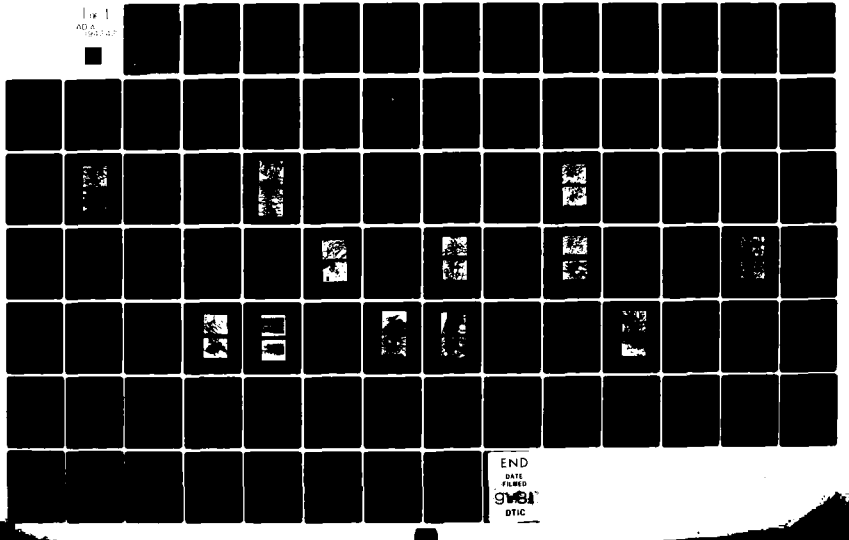

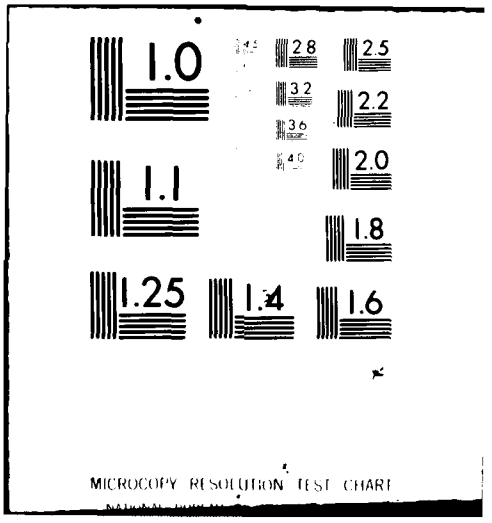
1.0
2.8
2.5
3.2
2.2
3.6
4.0
2.0
1.1
1.8
1.25
1.4
1.6
MICROCOPY RESOLUTION TEST CHART

AD A094242

(8)

INVESTIGATION OF CNTD MECHANISM AND ITS EFFECT ON MICROSTRUCTURAL PROPERTIES

LEVEL II

CONTRACT NO. N00019-78-C-0557

Report Prepared for:

U.S. Naval Air Systems Command

Washington, D.C.

Report Period - 9/20/78 to 9/20/79

Prepared By : Deepak G. Bhat, Ph.D.
Research Engineer

SAN FERNANDO LABORATORIES

Pacoima, California

Approved for public release; distribution unlimited

October, 1980

INVESTIGATION OF CNTD MECHANISM AND ITS EFFECT ON MICROSTRUCTURAL PROPERTIES

CONTRACT NO. N00019-78-C-0557

Report Prepared for:

U.S. Naval Air Systems Command

Washington, D.C.

Report Period - 9/20/78 to 9/20/79

Prepared By Deepak G. Bhat, Ph.D.
Research ~~Engineer~~

SAN FERNANDO LABORATORIES

Pacoima, California

Approved for public release; distribution unlimited

October, 1980

SECURITY CLASSIFICATION OF THIS PAGE (When Data Entered)

REPORT DOCUMENTATION PAGE	READ INSTRUCTIONS BEFORE COMPLETING FORM
1. REPORT NUMBER	2. GOVT ACCESSION NO. AD-A094 242	3. RECIPIENT'S CATALOG NUMBER
4. TITLE (and Subtitle) INVESTIGATION OF THE CNTD MECHANISM AND ITS EFFECT ON THE MICROSTRUCTURE AND PROPERTIES OF SILICON NITRIDE.	5. TYPE OF REPORT & PERIOD COVERED FINAL REPORT 9/20/78 to 9/20/79
	6. PERFORMING ORG. REPORT NUMBER
7. AUTHOR(s) D.G. Bhat Research Engineer	8. CONTRACT OR GRANT NUMBER(s) N00019-78-C-0557
9. PERFORMING ORGANIZATION NAME AND ADDRESS San Fernando Laboratories 10258 Norris Ave. Pacoima, CA 91331	10. PROGRAM ELEMENT, PROJECT, TASK AREA & WORK UNIT NUMBERS
11. CONTROLLING OFFICE NAME AND ADDRESS NAVAL AIR SYSTEMS COMMAND Washington, D.C. 20361	12. REPORT DATE October, 1980
	13. NUMBER OF PAGES 74
14. MONITORING AGENCY NAME & ADDRESS (if different from Controlling Office) DCASMA Van Nuys 6230 Van Nuys Blvd. Van Nuys, California 91408	15. SECURITY CLASS. (of this report) UNCLASSIFIED
	15a. DECLASSIFICATION/DOWNGRADING SCHEDULE

16. DISTRIBUTION STATEMENT (of this Report)

17. DISTRIBUTION STATEMENT (of the abstract entered in Block 20, if different from Report)

18. SUPPLEMENTARY NOTES

19. KEY WORDS (Continue on reverse side if necessary and identify by block number)

Silicon Nitride
Chemical Vapor Deposition
CVD
Grain Refinement

20. ABSTRACT (Continue on reverse side if necessary and identify by block number)

This report presents results of a research program in which we sought to develop a chemical vapor deposition (CVD) method for the deposition of extremely fine grained silicon nitride.

The program consisted of three separate technical efforts. The first effort, a parametric study of the conventional silicon tetrahalide-ammonia CVD chemistry, produced no significant grain refinement in the Si_3N_4 deposits.

DD FORM 1 JAN 73 1473 EDITION OF 1 NOV 65 IS OBSOLETE

SECURITY CLASSIFICATION OF THIS PAGE (When Data Entered)

The second effort attempted, with no success, to utilize silicon halide disproportionation chemistry in the CVD process. Finally, we observed an apparently successful Si_3N_4 grain refinement during the third effort in which we used the competing codeposition of separate phases to interrupt grain growth. During this effort, we tried the codeposition of silicon nitride and silicon carbide with no success. However, we found apparently good results when silicon nitride was codeposited with aluminum nitride.

TABLE OF CONTENTS

ACKNOWLEDGEMENTS

The work reported here was performed under Contract #N00019-78-C-0557 for the Department of the Navy, Naval Air Systems Command, Washington, D.C.

The author is grateful to Robert A. Holzl, President, San Fernando Laboratories for the initial guidance of the research, encouragement and numerous valuable discussions. Thanks are also due to Drs. Jacob Stiglich and Rodney M. Panos for valuable discussions and suggestions. The deposition work was performed by Messrs. Sam Rustomji, Gerald Galarneau, Clifford Lewis and Philip Kalkowski under the expert supervision of Benjamin Tilley. Ms. Colleen Murphy assisted in the compilation of experimental data.

LIST OF FIGURES

LIST OF FIGURES (Continued)

LIST OF TABLES

I. INTRODUCTION

The research and development group at San Fernando Laboratories has been engaged in an in-depth study of the characteristics of chemically vapor deposited silicon nitride for the past several years. A major effort in this regard was sponsored by the Department of the Navy (NAVAIR). A summary report, covering the activities of the first year which ended in July, 1978 was written under Contract No. N00019-77-C-0557. In the present report, we describe the results of the development work carried out in the second year of the program under Contract No. N00019-78-C-0557. This work concluded in September, 1979.

During the first year of effort, we concentrated on the study of various process parameters in the $SiCl_4/NH_3/H_2$ system. The objective was to define the deposition parameters that would result in a fine-grained, dense deposit of α-Si_3N_4 on resistively heated tungsten filaments. We discovered that the substrate temperature and the total pressure were the major variables which influenced the morphology of the deposit. We also found that it was possible to influence the morphology and grain size of the deposits by controlled additions of hydrocarbons to the gas stream. The measurements of flexure strength, hardness and fracture toughness (by the indentation technique [2]) yielded average values of 550 MPa (80 ksi), 2500-3500 HV_{500} and 3-5 $MPa\sqrt{m}$ respectively. Isolated values of strength and fracture toughness of 1000 MPa (145 ksi) and 7 $MPa\sqrt{m}$ suggested the potential of this material that could be realized by a better understanding and control of the

process parameters. We recommended that the efforts be continued to achieve this understanding and control, and also to attempt the deposition of translucent or transparent Si_3N_4 for possible use in electro-optical applications.

Thus, the objective of the effort during the second year was to carry out an extended parametric study of the silicon nitride deposition. Ultimately, we hoped to apply the technique of controlled nucleation thermochemical deposition (CNTD)* [3-5] to this material. Essentially, the CNTD process results in a deposit of extremely fine grain size, of the order of 500-1000Å, and superior mechanical properties. This process has been successfully applied to the tungsten-carbon system [3] and silicon carbide. [4-6] Other systems in which limited success was achieved in the application of CNTD include Ti-B and Zr-B.[5] The significant success with the CNTD process in the SiC system [6] prompted us to examine the possibility of extending the technique to the other Si based ceramic systems, such as Si_3N_4. As mentioned earlier, the efforts during the second year of the NAVAIR program were, therefore, directed towards this objective. These efforts are described in the following pages.

We divided the experimental work into a number of categories. In the first phase, efforts were made to establish process parameters under the condititions of indirect heating of the substrates in a furnace. Several variables were selected for study so as to define a set of conditions for the optimum deposition of Si_3N_4 with a given gas mixture.

*Process developed and patented by San Fernando Laboratories, a division of Dart Industries.

The second phase of the program was conducted concurrently with a similar program on the development of silicon carbide under the auspices of Air Force Office of Scientific Research (AFOSR). This work involved deposition of elemental silicon by the disproportionation of a lower halide and subsequently, conversion of silicon to SiC or Si_3N_4 using appropriate source.

In the third phase of this program, we attempted to co-deposit SiC to achieve grain refinement. We also studied the effect of "alloying" of Si_3N_4 by other compatible cations such as Al. It was expected that by setting up competitive reactions, it might be possible to prevent unilateral, columnar growth of any one specie, thereby effecting grain refinement. In the final stage of the program, several test bars were coated with Si_3N_4 for detailed evaluation of structure and properties.

II. EXPERIMENTAL PROCEDURE:

(a) Deposition of Si_3N_4.

The outline of the experimental effort for the second year was based primarily on the experience gained during the first years' work. Several goals were defined, as described below.

1. Parametric Study:

The first objective was to change the method of heating the substrate. During the first year, we used tungsten filaments which were heated by internal resistance in a "cold-wall" reactor. We decided to use graphite bend-bar type substrates which would be heated indirectly in a furnace. The advantages of the latter type

of arrangement are (i) easier scale up (ii) possibility of depositing on complex shapes, and (iii) no restrictions with regard to electrical conductivity. Thus, we modified the design of the reactor chamber to allow for the indirect heating of graphite substrate. Figure 1 shows the schematic arrangement of the deposition chamber. The graphite furnace was heated by induction by coils placed around the quartz envelope surrounding the furnace. A clamshell-type heater was incorporated on the upstream side to permit preheating of the gas stream. This arrangement was used to deposit conventional silicon nitride on the bend bar substrates, during the initial parametric study.

The parametric study was divided into several sets of experiments. These were (i) use of nitrogen as the carrier gas for $SiCl_4$ and NH_3, (ii) use of argon as the diluent gas with no nitrogren in the gas stream, and (iii) use of SiF_4 as the source of Si.

In the first set, viz. nitrogen as carrier gas for $SiCl_4$ and NH_3, a total of 32 runs were made in which the effect of various parameters was studied with respect to the rate of deposition and morphology of the crystallites deposited. The run conditions are given in Table A-1 of Appendix I. We examined the nature of Si_3N_4 deposits as a function of substrate temperature, total pressure, active gas partial pressure (AGPP), partial pressure of hydrogen and the throughput velocity of the gases at a constant ratio of $SiCl_4$ to NH_3 of 0.2 (except run #29, see Table A-1 Appendix I). The active gas partial pressure was calculated according to the stoichiometric proportion of the two species required to make a mole

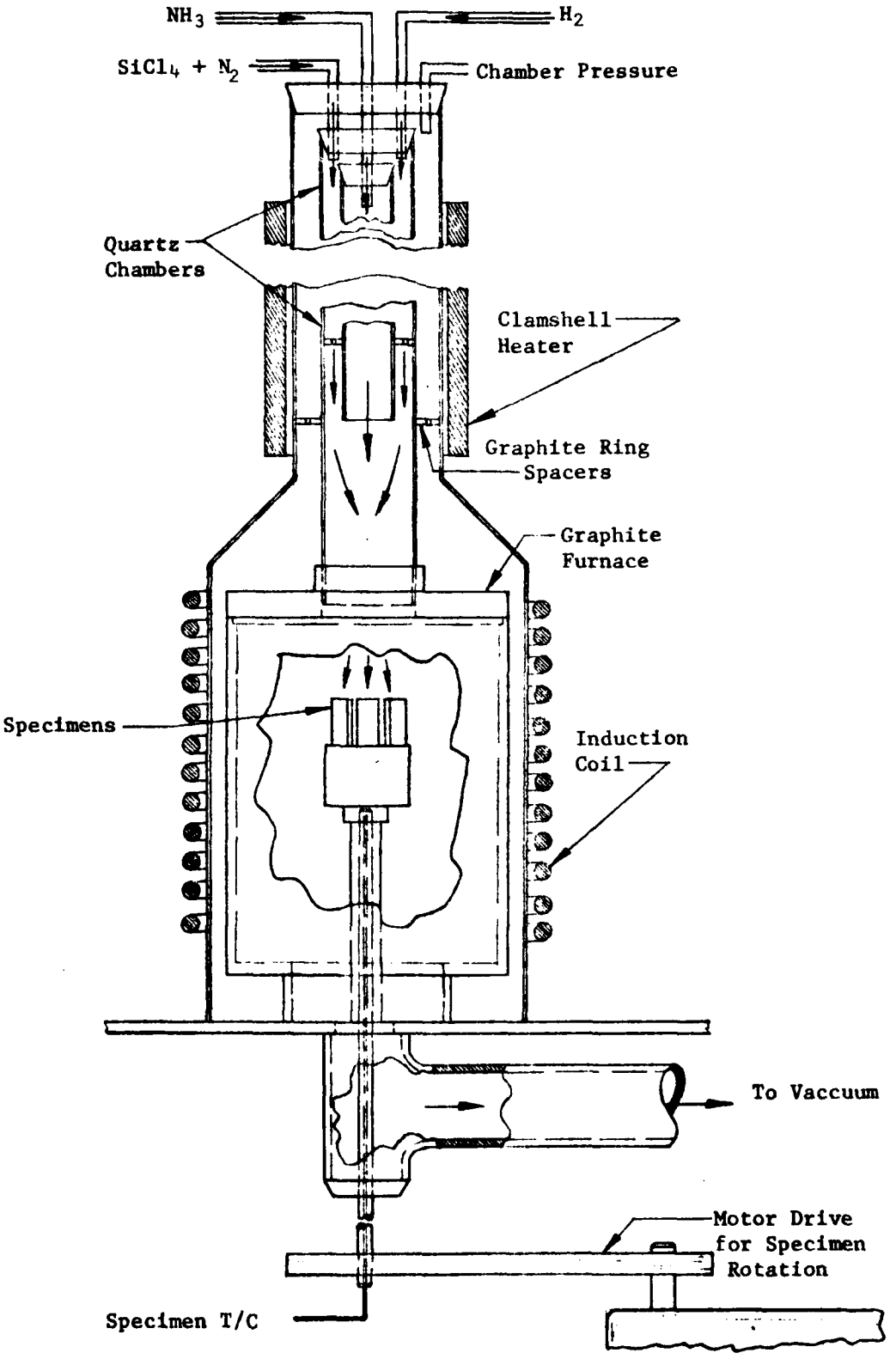

FIGURE 1 SCHEMATIC OF DEPOSITION CHAMBER FOR SILICON NITRIDE DEPOSITION IN A FURNACE.

of Si_3N_4. For example, in the reaction,

$$3\ SiCl_4 + 4\ NH_3 \rightarrow Si_3N_4 + 12HCl \qquad (1)$$

we need 4 moles of NH_3 for every 3 moles of $SiCl_4$ to make a mole of Si_3N_4. Thus the active gas concentration was obtained by adding the volumes of $SiCl_4$ and NH_3 in the proportion 3:4. Any excess of $SiCl_4$ or NH_3 was treated as such, and not included in the calculation.

In the second set of experiments, argon was used as a diluent gas. The variables were total pressure, substrate temperature, $SiCl_4/NH_3$ ratio, AGPP, partial pressure of hydrogen and the throughput velocity. A total of 15 runs were made. The run conditions are given in Table A-2, Appendix I.

Another useful source of silicon is SiF_4. Several runs were made with this precursor to study the effect of AGPP on the rate of deposition and properties of the deposit. The run conditions are summarized in Table A-3, Appendix I.

2. Silicon deposition by disproportionation of a subhalide:

For the second part of the effort, we used various methods for the deposition of elemental silicon. The reactor chamber was modified to accommodate a smaller chamber in which silicon bearing solid materials could be placed. The arrangement is shown in the schematic of Figure 2. The graphite pot, placed over the furnace

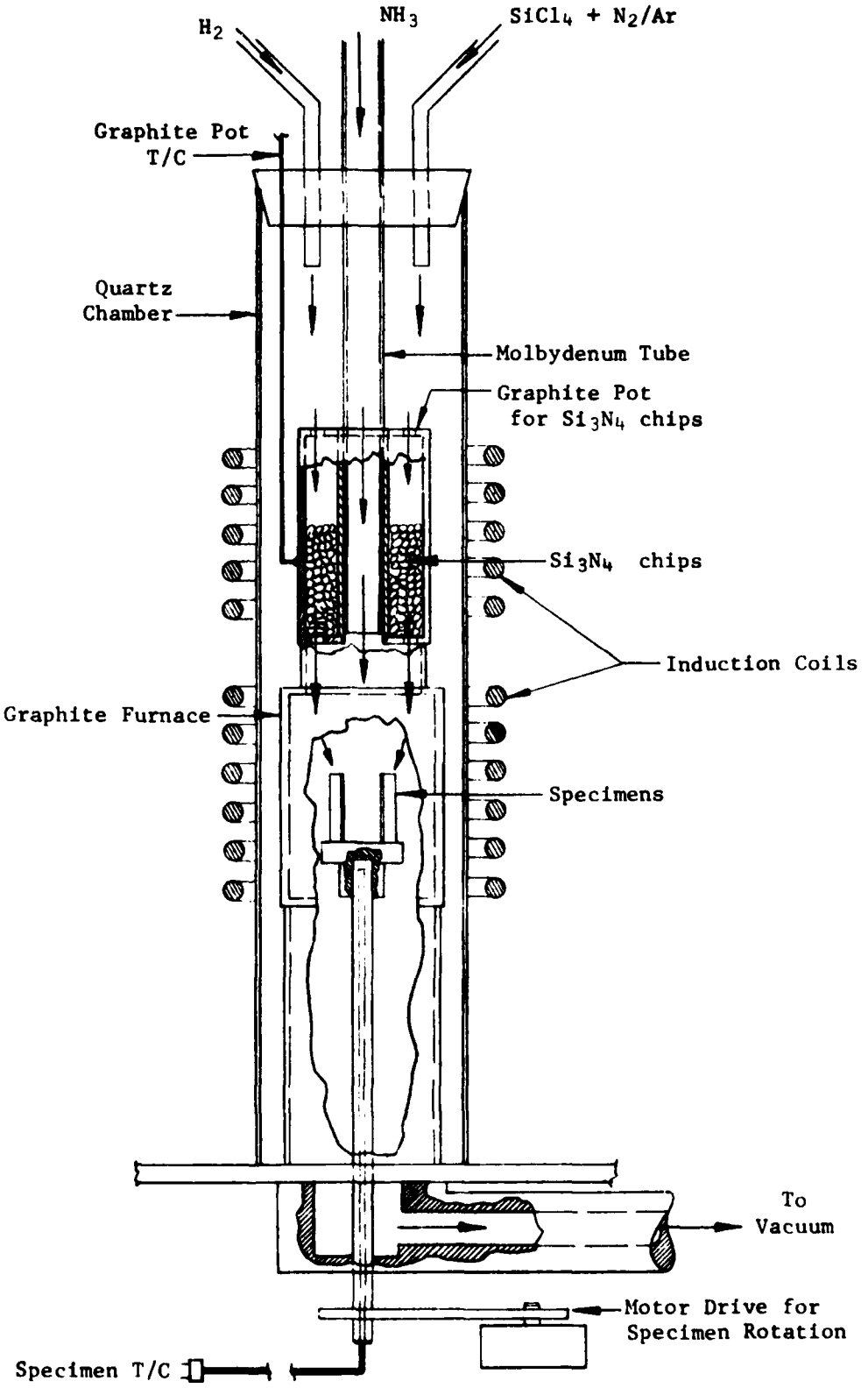

FIGURE 2 SCHEMATIC OF DEPOSITION CHAMBER FOR SILICON HALIDE DISPROPORTIONATION STUDY.

was used to hold semiconductor grade silicon chips or silicon nitride chips and scrap. The silicon bearing precursor gas was passed over this material to achieve the formation of a lower halide, which was subsequently disproportionated over the substrate in the furnace.

The initial experiments involving 12 runs were made under the AFOSR program. $SiCl_4$ was passed over hot silicon nitride scrap (mostly RBSN from different sources) and then allowed to enter the furnace to react with ammonia. These runs were then continued under the present contract and an additional 34 runs were made. In the last three runs, $SiHCl_3$ was used as the precursor gas in place of $SiCl_4$. The run conditions are summarized in Table A-4, Appendix I.

3. "Alloying" of Si_3N_4 for grain refinement:

This phase of the program was aimed at grain refinement by alloying. In this work, we first examined the effect of adding propane to the gas stream. The purpose was to study the possibility of carbonitriding of silicon and thereby attempt grain refinement in the deposit. Most of the nine runs were carried out at a constant temperature of 1375°C and a total pressure of 40 torr. The variables were hydrogen pressure, velocity of gases and amount of propane. In calculating the hydrogen pressure, the contribution of propane (4 moles of H_2 for each mole of propane) was taken into account. The method used in calculating the active gas partial pressure is discussed in the next section. The run conditions are given in Table A-5, Appendix I.

In an alternative approach to the same goal, four runs were made with methyltrichlorosilane (MTS) as a source of silicon. Again, the purpose of this brief set of runs was to examine the possibility of co-depositing SiC and Si_3N_4, since MTS is used for the deposition of SiC. We attempted a quick survey of the effect of substrate temperature, hydrogen pressure and total flow on the nature of the deposit. As discussed in the next section, the results were not encouraging, therefore, no further work was done. The run conditions are given in Table A-6, Appendix I.

We were examining the possibility of refining the grain structure of AlN by the introduction of Si on a concurrent program for Al development under the auspices of AFOSR.[13] These experiments gave encouraging results for AlN. Therefore we attempted to carry out similar experiments for introducing Al into Si_3N_4. While attempting to effect "alloying" of AlN by Si, we had made a brief attempt to do the same at the other end, i.e. "alloying" of Si_3N_4 by Al. These runs, included in this report (see Table A-7, Appendix I), gave encouraging results. Therefore, we continued this effort under this program.

The furnace design for these experiments is shown in Figure 3. The inner quartz chamber was used for aluminum granules. The chamber was heated by a clamshell heater placed round the outer quartz envelope. Aluminum was converted to $AlCl_3$ by reacting with HCl, and then introduced into the main gas stream near the furnace below. The deposition

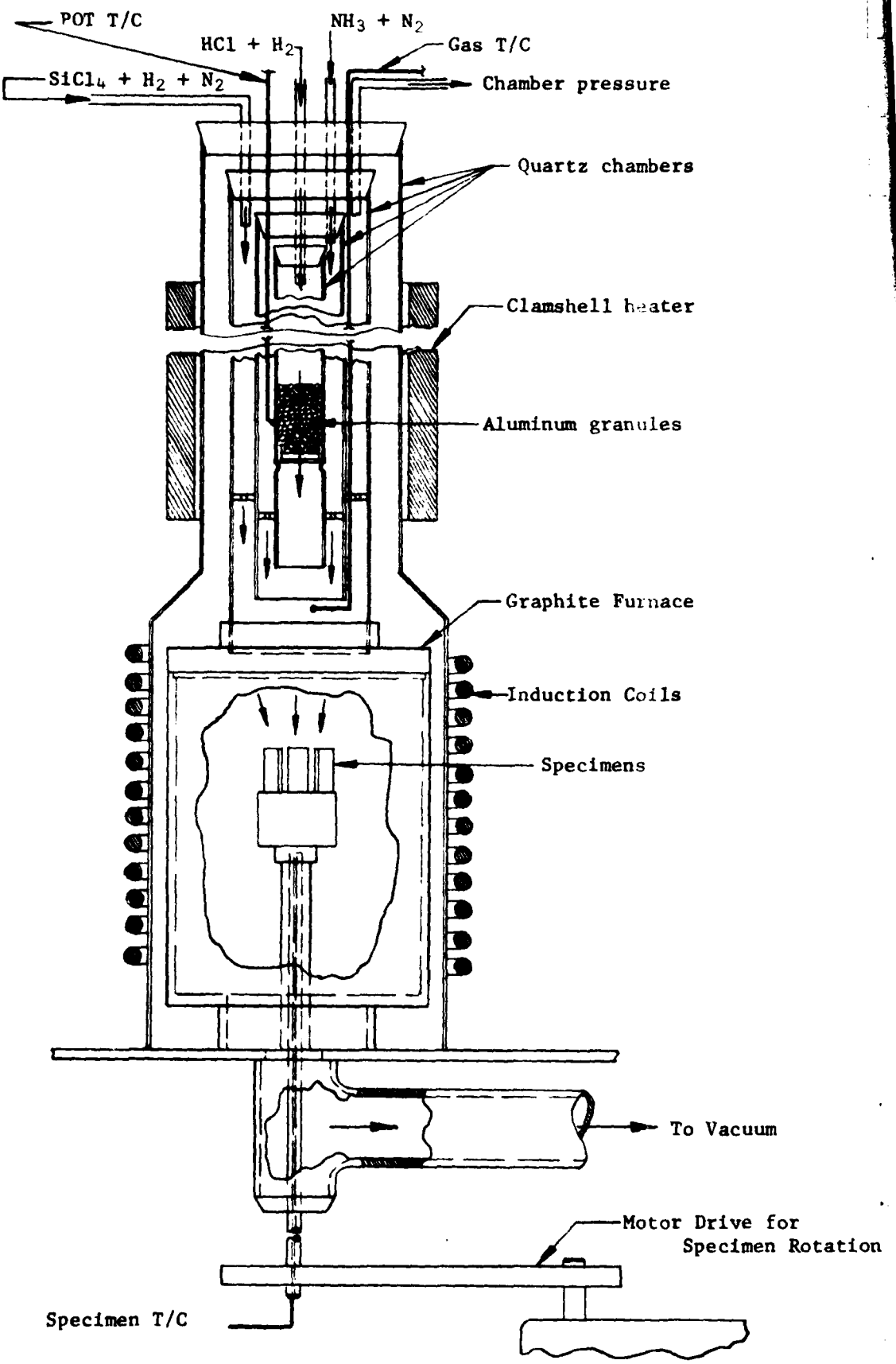

FIGURE 3 SCHEMATIC OF DEPOSITION CHAMBER FOR ALUMINUM "DOPANT" STUDY

parameters of these experiments are given in Table A-7, Appendix I.

4. Deposition of test bars:

Several test specimens were made by depositing Si_3N_4 on reaction bonded silicon nitride substrates. These samples were submitted to NAVAIR for evaluation and testing. The deposition conditions for these bars are shown in Table A-8, Appendix I.

(b) Evaluation of Si_3N_4 deposits.

The deposits of Si_3N_4 made in the various runs were characterized by different techniques. We used mechanical testing, microscopy (optical and SEM), X-ray diffraction and electron microprobe analysis. A brief description of the apparatus and procedure follows.

1. Transverse Rupture Strength (TRS) measurement

A table model mechanical testing machine made by Comten Corporation, St. Petersburg, Florida was used. The platen of the machine was fixed to a screw driven by a motor through a reduction gear train. The linear displacement rate of the machine platen was 1.27mm/min. Flexure testing was carried out in a three-point configuration. The fixture incorporated sintered tungsten carbide loading pins. The load at failure was displayed on a mechanical force gauge. We used mechanical force gauges (capacities 0-100 lbs. and 0-250 lbs.) instead of the hydraulic load cells since the former were more accurate and precise in the range of fracture loads encountered with deposits on graphite substrates. The standard test specimens were prepared by

depositing Si_3N_4 on graphite bend bars with dimensions 0.1" x 0.2" x 3.0" (nominal). Some RBSN bend bars, 0.125" x 0.25" x 3.0", coated with Si_3N_4 were also tested. The method of computation of the strength is given in Appendix II.

2. X-ray diffraction (XRD):

The crystallographic identification of the deposits was carried out on a General Electric XRD-5 unit at the University of Southern California. A nickel-filtered copper Kα radiation was used in all experiments, along with a 3^{o} diverging slit and a medium resolution 0.2^{o} receiving slit (Soller). Most of the work was done on as-deposited specimens, except in the case of very coarse-grained, rough deposits. These were diamond-ground to a flat finish using 70 micron grit. We also used some samples in a crushed powder form by grinding some deposit layers in an agate mortar. The samples were scanned through 15^{o} to 90^{0} 2θ and the patterns compared with those from ASTM card #9-250 of the Powder Diffraction File and with a computer-generated pattern developed by Gazzara and Reed.[8]

3. Scanning Electron Microscopy (SEM) and Energy Dispersive Analysis of X-rays (EDAX):

The electron microscopy work was performed on the deposits using an AMR 1200A SEM in our metallurgical laboratory. In addition, we used a Cambridge Stereoscan S4-10 SEM at the University of Southern California. The SEM examination was limited to an observation of as-deposited and fracture surfaces. Etched cross sections were not examined since we have not found a suitable room

temperature etchant for pure silicon nitride. A Tracor Northern EDAX system attached to the Cambridge SEM was used for the analysis of silicon content of the deposits. This information was semi-quantitative at best since the EDAX method is not amenable to the quantitative determination of light elements (Z<11).

4. Electron Probe Microanalysis (EPMA):

This technique provides a means of obtaining a fully quantitative chemical analysis. Samples from the "alloying" experiments were subjected to EPMA. The analysis was performed on an ETEC R1 SEM equipped with an Autoscan Crystal Spectrometer, at Scanning Electron Analysis Laboratories, Los Angeles. The operating conditions used are shown in Table I.

5. Hardness and Fracture Toughness

These properties were determined with the aid of a Leitz Miniload Microhardness tester using a Vickers diamond indentor. Hardness was measured at loads ranging from 100 to 500g. The fracture toughness was calculated from the measurement of the length of cracks generated by indentation. This technique is described by Evans and Charles.[2]

6. Electrical properties

The material made under this program was not used for the evaluation of electrical properties. However, these measurements were performed by an outside agency on silicon nitride deposits made under another program. Since San Fernando Laboratories did not participate

TABLE 1 OPERATING CONDITIONS FOR OBTAINING ELECTRON MICROPROBE DATA

Element	Accelerating Voltage, KV	Spectrometer Crystal*	Spectrometer Position, R	Detector Potential, KV	PHA** Setting	WD mm
Oxygen	10	RAP	3.6363	1.25	7.5 x 128	11
Nitrogen	10	LOD	1.2636	1.25	5x5 x 16	13
Chlorine	20	PET	2.1781	1.5	8.0 x 32	15
Aluminum	20	RAP	1.2856	1.5	7.5 x 16	15
Silicon	20	PET	3.2824	1.25	7.0 x 64	16

* RAP: Rubidium Acid Phthalate (d=13.0605Å)

LOD: Lead Stearate (d= 50.35Å)

PET: Pentaerythritol (d= 4.375Å)

** PHA: Pulse Height Analyzer Setting

in the evaluation, the details of the techniques were not available. The results were, however, made available to us through the courtesy of Mr. Leggett of Hughes Aircraft Company. These are included in the following section.

III RESULTS AND DISCUSSION

The study of the relationship between deposition parameters and the characteristics of the deposit was begun on the basis of some experience gained in the furnace deposition experiments conducted in a company funded IR&D program. This work was directed towards the deposition of high strength silicon nitride in thick sections using graphite substrates. Using the deposition parameters from this study, we started our effort in the present program. The results of the various experiments aimed at refining the grain size of the deposits are described below. The characterization involved examination of crystal morphology, deposition rate and mechanical properties such as hardness and fracture toughness. Several specimens were also tested for transverse rupture strength. The findings of these evaluations are described in the following:

(a) Parametric study:

This study was initiated with a set of parameters in which nitrogen was used as the carrier gas. Although thermodynamic calculations suggest that a reaction between $SiCl_4$ and N_2 in the presence of hydrogen should yield Si_3N_4 in the temperature range 1600-1700K (ΔG_f^o = -40 to -50 kcal/mol), experience has shown that this does not happen.

Kijima, et al [9] were able to grow αSi_3N_4 whiskers in the temperature range 1675-1775°K at 1 atm. total pressure when they maintained a high nitrogen partial pressure (>0.5 atm.) and using very high purity gases containing less than 10 ppm oxygen and 0.5 ppm H_2O. At lower temperatures polycrystalline or amorphous deposits were obtained. In our experiments, we used nitrogen principally to adjust the throughput velocity of the gases. Table 2 gives the values of various deposition parameters in this set of experiments.

The total chamber pressure was varied between 25 torr and about 60 torr. The low pressure conditions were achieved by connecting the system to an aspirator. Thus, minor changes in chamber pressure occurred around a set value depending upon the barometric pressure and ambient temperature fluctuations. Then, the experiments may be divided into four sets in which the chamber pressure was maintained in a given range, e.g. 25-30 torr, 39-42 torr, 45-55 torr and 58-62 torr. Within each set, we examined the effects of other parameters such as the active gas partial pressure (AGPP), partial pressure of hydrogen and gas velocity on the deposition rate. The method of calculation of AGPP was described in the previous section. The velocity of the gases was corrected for chamber pressure and substrate temperature. Except for one run, the $SiCl_4/NH_3$ ratio was held constant at 0.2.

When the variation of deposition rate was examined as a function of other parameters within a given set, we could not find any systematic correlation. An examination of Table 2 shows that the deposit morphology also appeared to be unrelated to any given parameter.

TABLE 2 Summary of results on Si_3N_4 made with nitrogen as carrier gas

Run #	Total Pressure Torr.	Substrate Temp. °K	AGPP Torr.	P* H Torr	Gas Velocity at T&P M/S	$SiCl_4$/NH_3 Ratio	Deposition rate μm/hr	HV 200 kg/mm²	K_c MPa$\sqrt{m}$	TRS 3 point MPa(ksi)	Remarks
1-1	25	1635	0.53	3.0	23.2	0.2	78				Uniform, fine grained deposit.
1-2	25	1575	0.53	3.0	22.3	0.2	78				-
1-3	25	1500	0.53	3.0	21.3	0.2	-				Fine grained deposit with some large growth spots - clear crystallites.
1-4	25	1500	1.10	6.3	10.6	0.2	-				Coarser grains than previous run, some tendency for whisker-like growth in few areas.
1-5	26	1650	0.36	2.1	33.8	0.2	48				Clear, fine grained deposit, some spikes.
1-6	39	1650	0.30	1.7	41.8	0.2	48				As above, but no spikes.
1-7	52	1650	0.30	1.7	41.8	0.2	48				Clear, fine grained deposit.
1-8	52	1650	0.30	1.7	41.8	0.2	66	2750	2.95		Clear crystalline deposit- some spikes - RBSN substrate.
1-9	48	1620	0.27	1.7	44.5	0.2	48				-
1-10	64	1650	0.29	1.6	43.8	0.2	36	2800	2.6		Fine crystals and spikes, cracks on top. RBSN substrate.
1-11	60	1680	0.27	1.5	47.4	0.2	18				Fine grained clear deposit.
1-12	66	1725	0.30	1.6	44.4	0.2	60				As above, some green coloration in the crystals.
1-13	25	1635	0.53	3.0	23.2	0.2	66	2770	3.35	85.5 (12.4)	Fine crystallites, some spikes. RBSN substrate.
1-14	40	1650	0.30	1.7	40.8	0.2	102	2725	4.6	152.0 (22.0)	Fine grained and clear, transparent deposit, some spikes. RBSN substrate.
1-15	52	1700	0.30	1.7	43.1	0.2	96				-
1-16	55	1650	0.32	1.8	39.5	0.2	24				Poor adhesion to substrate no spikes, fine deposit.
1-17	62	1650	0.36	2.0	35.1	0.2	54				Adhesion is better, fine dark crystals.
1-18	61	1700	0.36	2.0	36.7	0.2	36				Dark crystalline deposit on top, white crystalline on rest of the bar.
1-19	58	1750	0.33	1.9	39.8	0.2	72				As above.
1-20	58	1800	0.33	1.9	40.9	0.2	-				As above, bottom shows poor adhesion.
1-21	59	1650	0.33	1.9	36.8	0.2	-				Very thin deposit with a fine crystallite size.
1-22	45	1650	0.34	2.0	36.2	0.2	66				As above.
1-23	47	1650	0.36	2.0	34.7	0.2	-				Clear, thin deposit.
1-24	78	1650	0.64	3.7	39.1	0.2	150				-
1-25	48	1650	0.45	2.6	34.8	0.2	-				Thin deposit, partly crystalline.
1-29	28	1525	1.14	7.3	22.1	2.9	-				Poor adhesion of deposit.
1-35	41	1645	0.33	1.9	47.8	0.2	48				Strong (102) orientation, fine dark crystalline deposit. EDAX: 60.5 w/o Si.
1-36	40	1645	0.33	1.8	49.0	0.2	-				Coarse(20-200μm)crystallites on fine grained (1μm) matrix.
1-37	42	1645	0.33	6.7	46.6	0.2	90				-
1-38	40	1645	0.60	3.4	26.1	0.2	60				-
1-58	47	1650	0.38	24.0	40.9	0.2	36				Dark, medium grain size deposit.
1-59	47	1775	0.38	24.0	44.0	0.2	180	2890	4.1	450 (65.2)	10-15 μm crystallite size, some large crystals. EDAX: 61.8 w/o Si and 0.1 w/o Cl, strong (322) and (222) orientation.

A typical chemical vapor deposition system contains several variables such as total pressure, partial pressures of various gases, gas temperature, gas composition, substrate temperature etc. These parameters are usually interdependent. In addition, in many systems such as Si_3N_4, there are reactions in the gas phase that are not fully understood. Thus, in our system, it was usually difficult to control these variables in a perfectly reproducible manner. These difficulties probably resulted in the range of crystal morphologies described in Table 2 for seemingly similar deposition conditions.

Secondly, the deposition rates, measured by determining the coating thickness, were subject to considerable error especially when rough deposits were obtained. Very often, the deposits did not adhere to the substrate, and no measurements could be made. However, these findings pointed out the need for a much better control of process parameters, especially the gas composition, before any correlation could be attempted. Experience gained in other programs also suggested that in a furance deposition process, very often the furnace walls would also be coated. This would then significantly affect the heat transfer in the gas stream from one run to the next.

We were successful in making fine grained Si_3N_4 deposits as shown in Table 2. An example of the crystal morphology is shown in Figure 4. The size of the crystalliets varied widely, even within a given sample. For example, the crystallite size in Figure 4a is between 2 and 10μm, while in Figure 4b, it varies from about 10 to 100μm. Mechanical

A

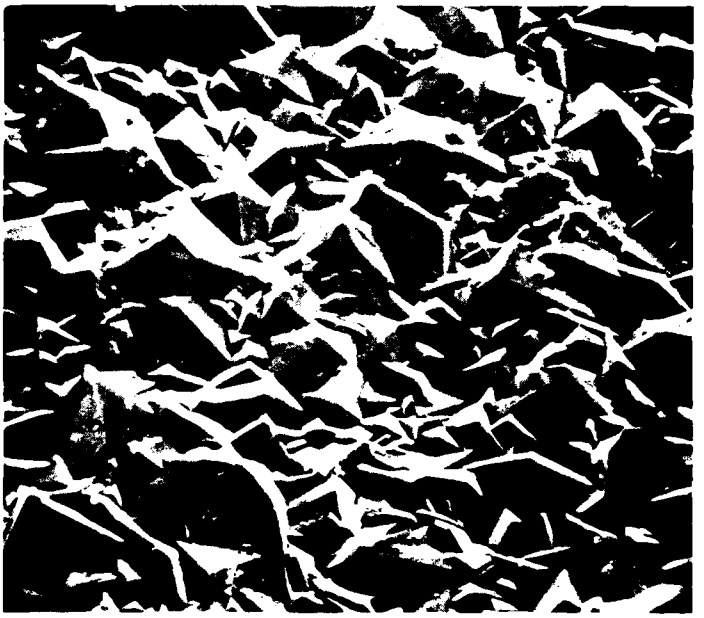

B

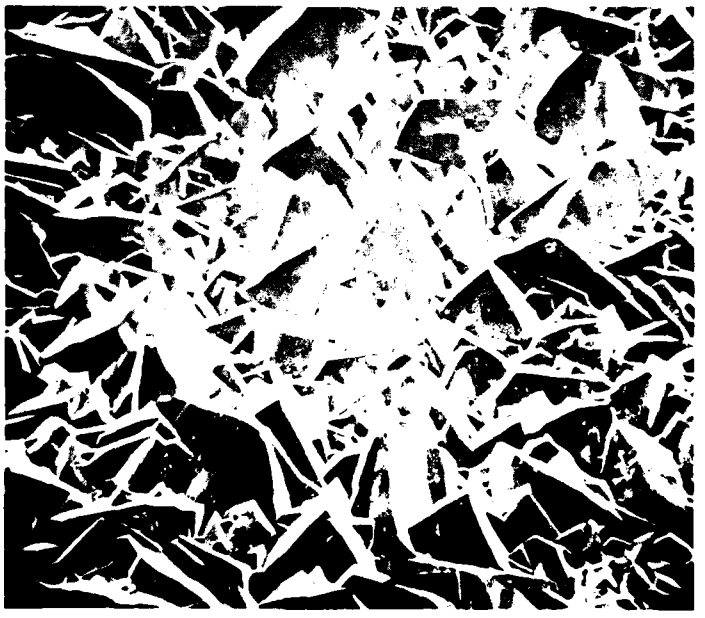

FIGURE 4 Morphology of Si_3N_4 made with nitrogen as the carrier gas.

A) 2000X

B) 200X

property evaluation of some of the deposits gave reasonable results. Hardness values ranged from 2700 to 2800 (HV_{200}) and fracture toughness from 2.6-4.6 $MPa\sqrt{m}$. As shown in Table 2, the deposits were usually oriented, with no particular orientation consistently dominant from sample to sample. EDAX analysis for Si and Cl contents revealed that the deposits were probably stoichiometric in silicon. For pure silicon nitride the stoichiometric proportions of Si and N are 60 w/o and 40 w/o respectively. Some samples showed the presence of small amount of chlorine. It is not clear if the presence of chlorine is due to residual, unreacted silicon halide, and whether chlorine is present at the crystallite boundaries. Since EDAX cannot detect nitrogen or oxygen, it is not clear if all the silicon is tied up with nitrogen or whether some SiO_2 may also be present.

Attempts to correlate deposition rates with process parameters for specimens made with argon as the diluent gas were also unsuccessful. The various parameters are shown in Table 3. The pressure was maintained at 25-30 torr and the velocity of gases was maintained, in one set, at 21-25 m/s. The variable in this set was the $SiCl_4/NH_3$ ratio, with AGPP at 1.2 ± 0.1 torr and hydrogen partial pressure at 6.5-7.5 torr. Again, there was no correlation possible.

Microscopic evaluation of deposits in this set showed a wide variety of deposit of morphologies - from highly oriented whiskerlike growth to fine, equiaxed crystallites. Figure 5 shows an example of the range of morphologies obtained. Most samples showed a crystal morphology similar to that in Figure 5a. However, in some areas of the coating in a given sample, a very fine grained deposit was obtained, as shown

TABLE 3 Summary of results on Si_3N_4 made with argon as the diluent gas

Run #	Total Pressure Torr.	Substrate Temp. °K	A GPP Torr.	P H_2 Torr.	Gas Velocity at T&P M/S	$\frac{SiCl_4}{NH_3}$ ratio	Deposition rate μm/hr	HV_2 kg/mm (Load)	K_c $MPa\sqrt{m}$	TRS 3 point MPa (ksi)	Remarks
1-26	28	1525	1.10	7.3	22.1	2.9	204				Coarse crystallites.
1-27	25	1525	1.70	6.4	24.7	1.8	126				Fine, opaque crystals.
1-28	25	1520	0.88	6.5	24.6	3.6	-				Preferential growth of spikes due to heterogeneous nucleation on the matrix of fine crystals.
1-30	28	1525	1.14	7.3	22.1	2.9	-				Poor deposit, whisker growth, white needles - appear amorphous.
1-31	28	1475	1.14	7.3	21.4	2.9	-				Mixed amorphous type and crystalline deposit.
1-32	28	1475	1.30	7.3	21.4	2.75	360				Clear, coarse crystallites.
1-33	28	1475	1.30	7.3	21.4	2.75	156				Coarse, amber crystallites which appear transparent.
1-34	28	1425	1.30	7.3	20.6	2.75	102				Clear amorphous deposit.
1-39	67	1650	0.55	3.1	45.5	0.2	126	3210 (200)	3.55		Deposit on a vertical disc, uniform, fine deposit. Analysis (EDAX) shows 60.7 w/o Si, 0.2 w/o Cl
1-40	67	1645	0.55	1.7	45.4	0.2	126				Mixed crystal size along the periphery of disc. Range 10-12 μm-shows strong (002) orientation in XRD.
1-41	29	1645	1.35	7.5	86.2	2.75	300				as above
1-42	29	1545	1.35	7.5	81.0	275	-				-
1-43	28	1525	0.80	4.4	35.9	2.75	186				-
1-44	28	1535	0.80	4.4	36.1	2.75	-				Strong (222),(322) and (304) orientations, Coarse (20μm) crystals and large spikes. Poor adhesion.
1-45	50	1625	0.72	4.0	42.8	2.75	102	2930 (100)			Coarse (15-20μm) crystallites on fine matrix. Amorphous white deposit on top. Matrix crystals 0.5-1μm.

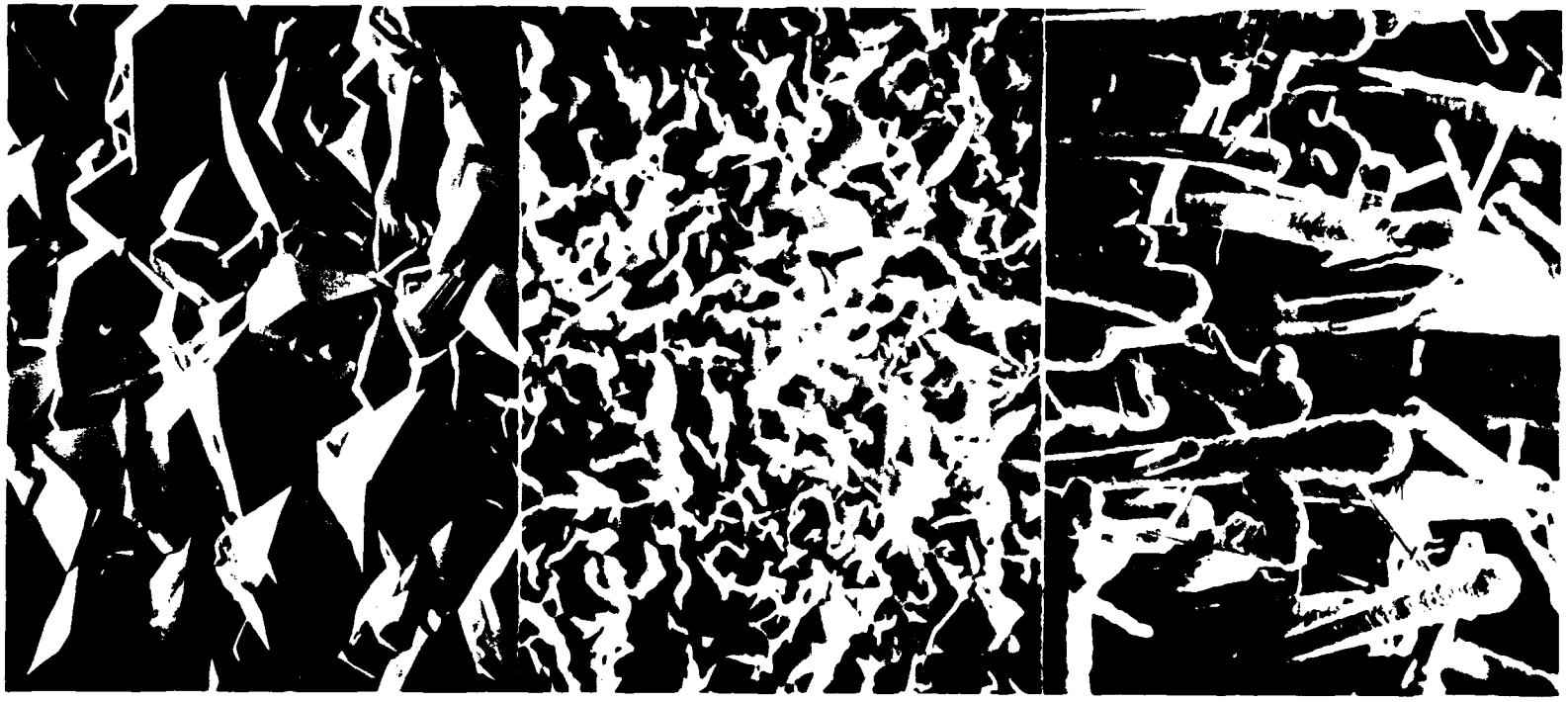

FIGURE 5 Various crystal morphologies of Si_3N_4 with argon as the diluent gas.

in Figure 5b. The average crystal size in this photograph is less than 1μm. In one sample, long whiskers of the type shown in Figure 5c were obtained on support rods. The fine crystal facets on individual needles suggest the possibility of a very fine grain size. Again, the lack of correlation of process parameters with deposit characteristics must be attributed to the difficulties in controlling the reactions in the chamber.

It is of interest to examine the $SiCl_4/NH_3$ system. The reaction

$$3SiCl_4 + 4NH_3 \rightarrow Si_3N_4 + 12HCl \qquad (1)$$

shows a change in the standard free energy of formation of 9,136 cal/mol at 500K.[10] Thus, the reaction, if it were allowed to occur, would theoretically be complete at a very low temperature. In reality, however, the tendency for the reactants is to form an intermediate product, silicon di-imide, $Si(NH)_2$. Nihara and Hirai[11] have suggested the following sequence of events:

$$SiCl_4 + 6NH_3 \rightarrow Si(NH)_2 + 4\ NH_4Cl$$

$$6\{Si(NH)_2\}_n \xrightarrow{675^oK} 2\{Si_3(NH)_3N_2\}_n + 2NH_3 \qquad (2)$$

$$\xrightarrow{925K} 3\{Si_2(NH)N_2\}_n + NH_3 \xrightarrow{1475K}$$

$$2Si_3N_4 + NH_3$$

Another mechanism that has been suggested is [12]

$$SiCl_4 + NH_3 \rightarrow SiCl_3NH_2 + HCl$$

$$SiCl_3NH_2 + SiCl_4 \rightarrow Si_2NHCl_6 + HCl$$

or

$$SiCl_3NH_2 + NH_3 \rightarrow Si(NH_2Cl)_2 + HCl$$

These intermediate species undergo further interactions by successive collisions and form more complex intermediate molecules containing increasing number of N atoms. In these reactions HCl is believed to be eliminated successively in the vapor phase before the gases reach the substrate surface where formation of Si_3N_4 is believed to occur. Lin [13], in his mass-spectrometric investigation of the intermediates in the $SiCl_4$-NH_3 system detected the presence of $SiNH_2Cl_2^+$ ions and several other ions.

In any case, whatever the mechanism of intermediate reactions, it is clear that these events occurring in the vapor phase are difficult to control since they depend on intermolecular collisions. Therefore we decided to explore the possibility of using SiF_4 as a source of silicon. While $SiCl_4$ and SiF_4 are very similar in chemical nature, their reactivities are quite different. The most important ions derived from the first combination of two reactants are similar in $SiCl_4$-NH_3 and SiF_4-NH_3 systems,[13] but the successive collision products are quite different. The higher reactivity of the chloride appears to

accelerate the formation of intermediate polymeric molecules containing several NH and NH_2 groups while in the fluoride system ions containing more than one NH_2 groups are not observed. [14] Thus, it might be possible to minimize the vapor phase reactions in the SiF_4-NH_3 system and achieve a better control of the deposition process.

The results of experiments made with SiF_4 precursor are shown in Table 4. Again, we encountered problems in correlating deposition parameters and deposition rates. Some indications were, however, obtained that the rate increased with substrate temperature but decreased with an increase in the AGPP, other conditions being identical. Very often, the measurement of deposition rate was rendered difficult due to non-uniform coating thickness along the length of the bar. This clearly suggested the possibility of non-uniform temperature and gas composition along the axis of the reactor. Another problem which could contribute to this variation was deposition on the furnace walls.

The mechanical characterization of the deposits was more extensive than in the previous sets. Hardness values ranged from about 2500 to 3150 (HV_{500}) and the fracture toughness was 3.6-5.0 MPa$\sqrt{m}$. The flexure strength values were between about 80-210 MPa, obtained on bars tested in an as-deposited conditions. Figure 6 shows a typical deposit made with SiF_4 precursor. In one case a crystalline deposit of an average size between 5 and 10 microns is obtained (Figure 6a). The formation of powdery surface layers is shown in Figure 6b. This particulate matter appeared to be adherent to the matrix surface.

TABLE 4

Summary results on Si_3N_4 made with SiF_4 as silicon source

Run #	Total Pressure Torr	Substrate Temp. °K	AGPP Torr.	P_{H_2} Torr.	Gas Velocity at T&P m/s	SiF_4/NH_3 Ratio	Deposition Rate μm/hr	HV Kg/mm^2 (average)	K_c $MPa\sqrt{m}$ (average)	(4 pt) MPa Ksi	Remarks
16-78	40	1775	0.65	20	37.0	0.13	245	2885	3.6	-	Fine crystalline deposit with tan and dark crystals.
16-79	40	1725	0.65	20	36.0	0.13	169	3150	4.0	-	Fine, clear crystallites.
16-80	40	1725	0.65	20	36.0	0.13	178	2830	4.0	-	Fine, dark crystallites.
16-81	40	1775	1.2	20	37.0	0.24	216	2490	3.9	79 (11.4)	Dark crystalline deposit, fine at top and coarse at bottom of bar.
16-82	60	1775	1.8	30	24.7	0.24	237	2790	4.8	200 (29.0)	Mixture of dark and light crystallites.
16-83	80	1775	3.6	30	18.5	0.37	229	2665	4.5	207 (30.0)	Mixture of dark and light crystallites.
16-84	40	1775	2.4	19.6	37.6	0.49	195	2770	5.0	-	Mixture of dark and light crystallites.
16-85	40	1875	2.4	19.6	40.0	0.49				-	Run stopped due to failure of vacuum system.
16-86	80	1875	2.4	40	39.6	0.49	288	2775	4.5	-	Non-uniform deposit, coarse crystallites on top.
16-87	80	1875	4.6	38.4	41.0	0.49	245	2605	4.8	-	Coarse crystallites ranging in color from white to black.
16-88	80	1875	4.6	38.4	41.0	0.49	474	2725	5.0	-	Uniform crystallites, dark.
16-89	80	1875	4.6	38.4	41.0	0.49	372	2770	4.7	157 (23.0)	Uniform crystallites, dark.

A

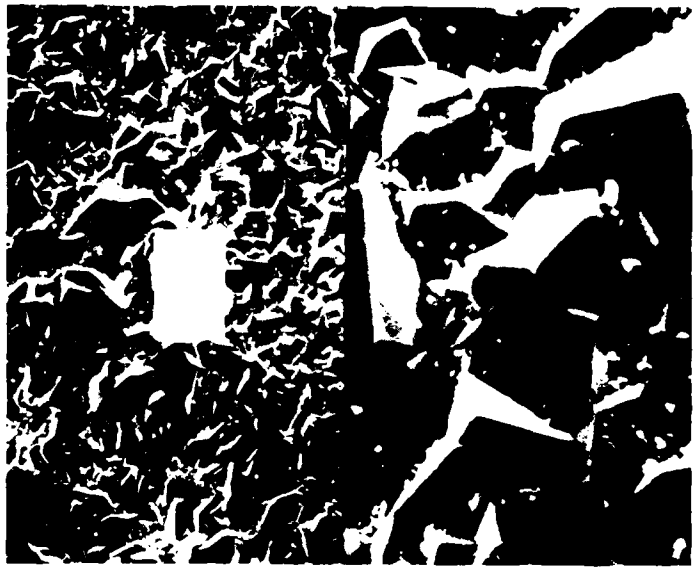

B

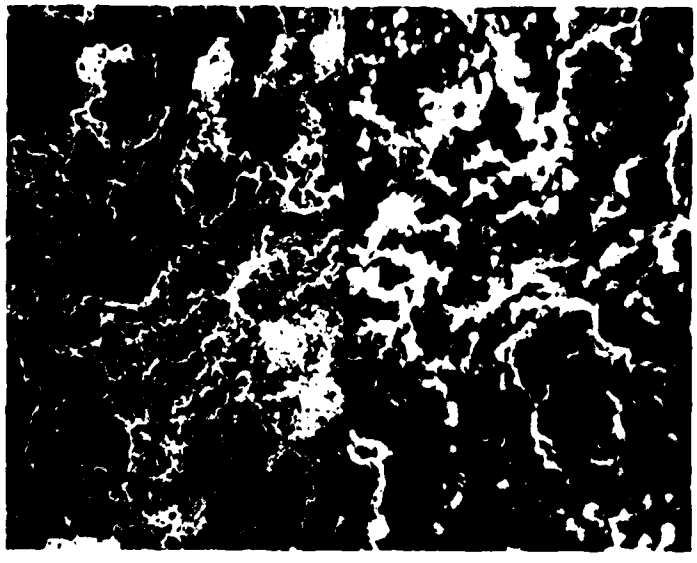

FIGURE 6 Morphology of Si_3N_4 made with SiF_4 as silicon source.

A) 500X/2500X

B) 500X/2500X

(b) Silicon deposition by disproportionation of a subhalide

The experiments described earlier were not successful in making a CNTD deposit of Si_3N_4. The nature of the CNTD process tends to suggest that an intermediate, polymeric product might be required [5] to achieve the grain refinement. While $SiCl_4$ might readily lend itself to such a reaction, its high reactivity to ammonia makes it difficult to control the reaction near the substrate surface, rather than in the gas stream.

Rochow [15] has shown that a reaction between $SiCl_4$ and H_2 may lead to the formation of an intermediate subhalide with an approximate composition $SiCl_{2.61}$. This precursor is believed to lead to the formation of CNTD silicon carbide. [4,5] At this point it became obvious to us that the conventional CVD system was probably not suitable for the grain refinement of Si_3N_4. We, therefore, sought alternative approaches to the conventional one. One possibility was to deposit elemental silicon and then attempt its nitridation.

While it may be possible to deposit elemental silicon by a variety of methods using different precursors, it appeared to be appropriate to use the same basic system of $SiCl_4$-H_2 or $SiHCl_3$-H_2 that we had extensively used in our investigations of silicon ceramics. Also, there were potential advantages in depositing silicon by first forming a subchloride and disproportionating the same over a substrate. The most obvious potential benefit was grain refinement if the disproportionation could be carried out simultaneously with nitridation.

We studied the feasibility of this approach for the following reactions:

$$SiCl_4(g) + Si(s) \rightarrow 2\ SiCl_2(g) \qquad (4)$$

$$2SiHCl_3(g) + Si(s) \rightarrow 3SiCl_2(g) + H_2(g) \qquad (5)$$

The lower halide is produced by passing $SiCl_4$ or $SiHCl_3$ over hot semiconductor grade silicon chips in a graphite crucible. The variation of the standard free energy change of the reactions with temperature for the silicon chip crucible is shown in Figure 7.

The equilibrium constant of the reaction, $K = \exp(-\Delta G/RT)$, can also be expressed in terms of composition and total pressure, and, for the two reactions considered above is given by:

$$K_4 = \frac{n^2_{SiCl_2}}{n_{SiCl_4}} \left[\frac{P}{n_{SiCl_2} + n_{SiCl_4} + n_I}\right] \qquad (6)$$

$$K_5 = \frac{n^3_{SiCl_2} \cdot n_{H_2}}{n^2_{SiHCl_3}} \left[\frac{P}{n_{SiCl_2} + n_{H_2} + n_{SiHCl_3} + n_I}\right]^2 \qquad (7)$$

Where n_i is the number of moles of the i^{th} species, n_I is the number of moles of the inert (carrier) gas(es) and P is the total pressure. Using these expressions, the equilibrium degree of completion of the reactions was determined for different values of the parameters n_I/n_R and P where n_I/n_R = the ratio of the moles of inert gas to the moles of reactant gases, or the degree of dilution of the gases. The results are plotted in Figure 8 and 9.

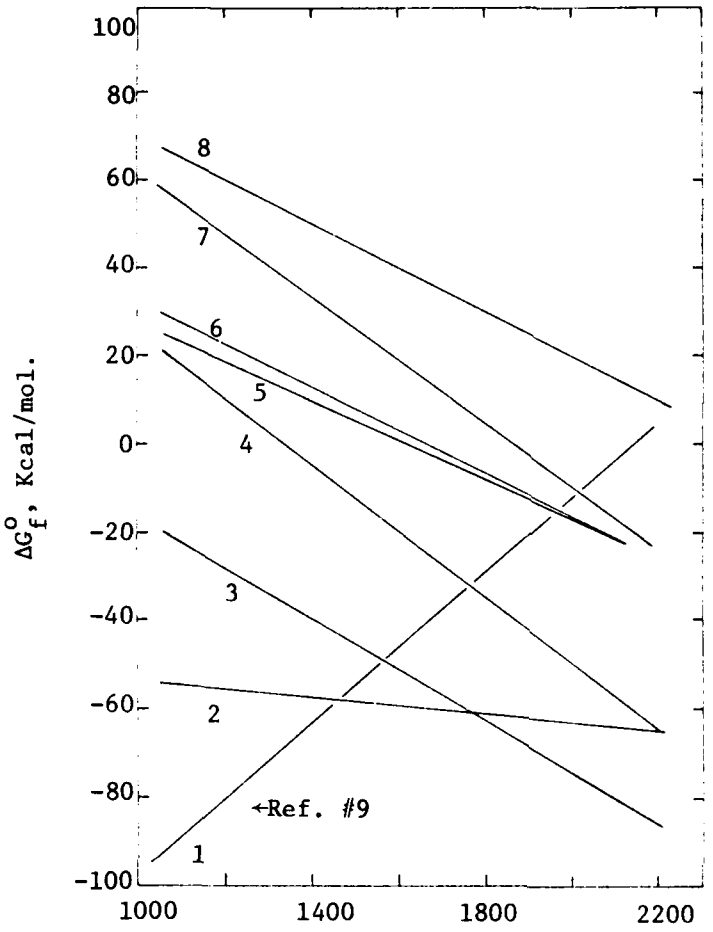

1. $3Si(s) + 2N_2(g) \rightarrow Si_3N_4(s)$ Ref. #9
2. $Si(s) + \frac{4}{3} NH_3(g) \rightarrow \frac{1}{3} Si_3N_4(s) + 2H_2(g)$
3. $SiCl_4(g) + \frac{4}{3} NH_3(g) \rightarrow \frac{1}{3} Si_3N_4(s) + 4HCl(g)$
4. $2SiHCl_3(g) + Si(s) \rightarrow 3SiCl_2(g) + H_2(g)$
5. $SiCl_4(g) + Si(s) \rightarrow 2SiCl_2(g)$
6. $SiF_4(g) + \frac{4}{3} NH_3(g) \rightarrow \frac{1}{3} Si_3N_4(s) + 4HF(g)$
7. $SiCl_4(g) + \frac{1}{3} Si_3N_4(s) \rightarrow 2SiCl_2(g) + \frac{2}{3} N_2(g)$
8. $SiF_4(g) + H_2(g) \rightarrow SiF_2(g) + 2HF(g)$

FIGURE 7 FREE ENERGY OF FORMATION AS A FUNCTION OF TEMPERATURE FOR VARIOUS REACTIONS.

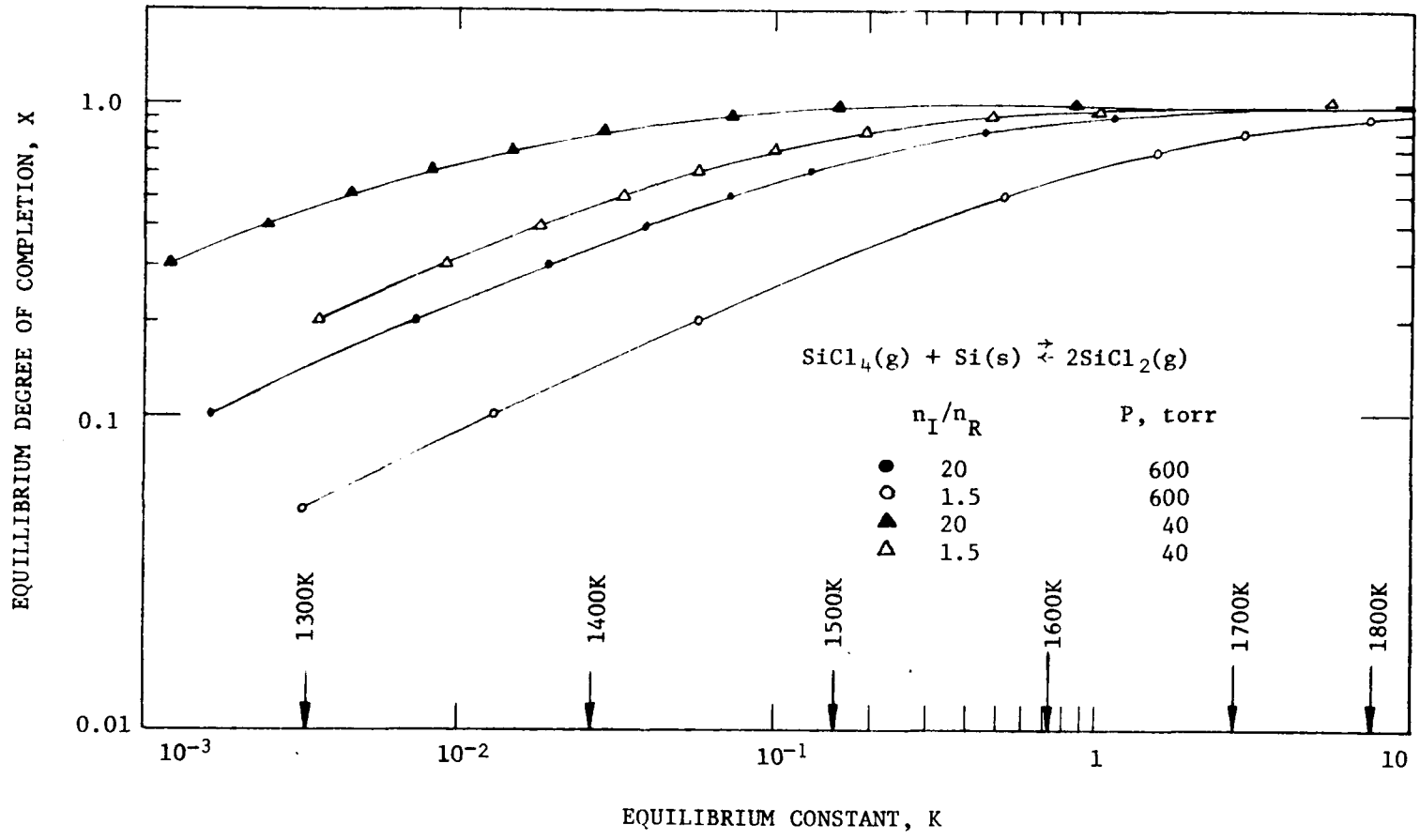

FIGURE 8 EQUILIBRIUM DEGREE OF COMPLETION OF $SiCl_4$ REDUCTION AS A FUNCTION OF TEMPERATURE, PRESSURE AND DEGREE OF DILUTION.

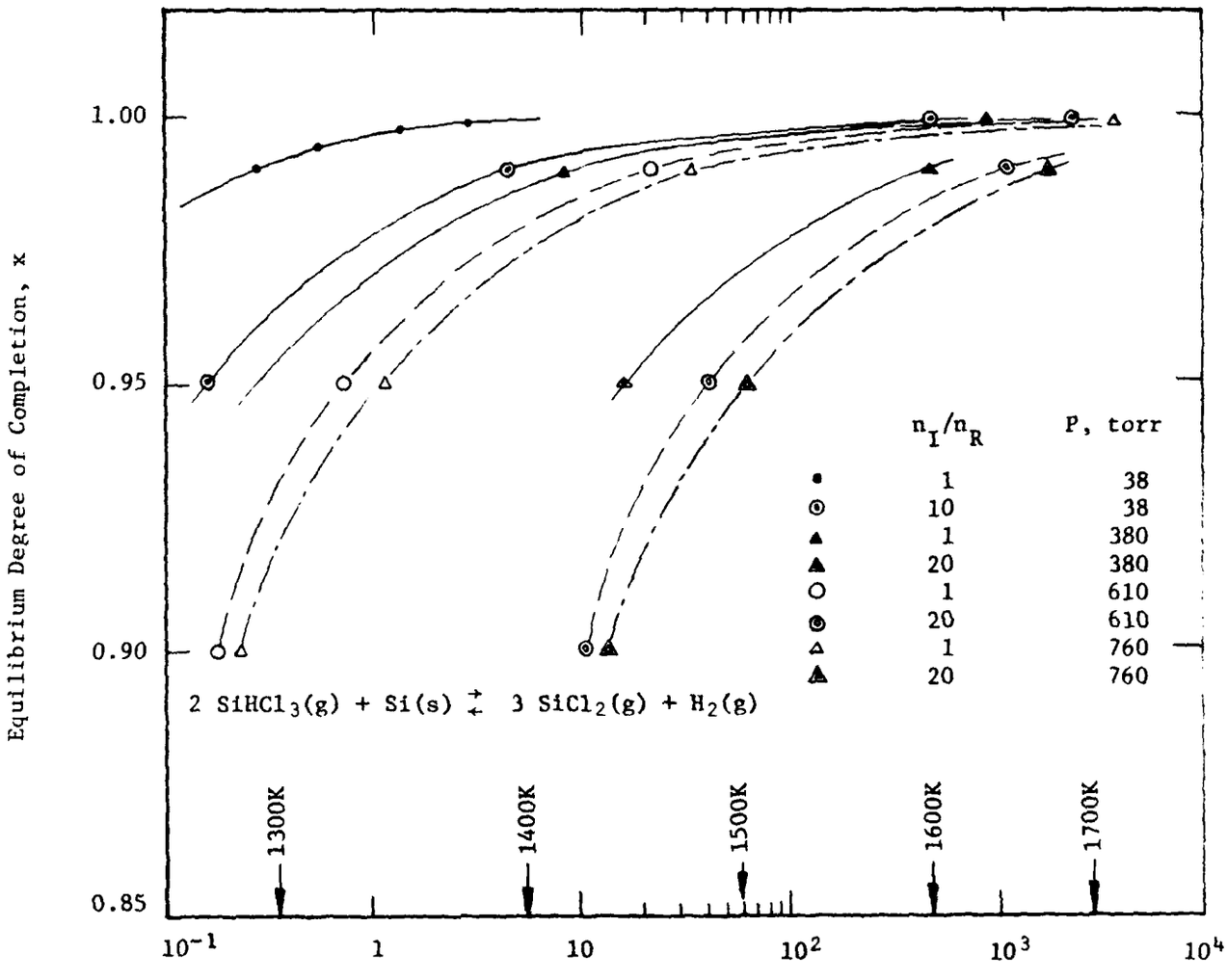

FIGURE 9 EQUILIBRIUM DEGREE OF COMPLETION OF $SiHCl_3$ REDUCTION AS A FUNCTION OF TEMPERATURE, PRESSURE AND DEGREE OF DILUTION.

Considering reaction (4), it is clear that a substantial amount of $SiCl_2$ can be generated above 1500°K if the total pressure is reduced to 40 torr and sufficient dilution of the gas stream is carried out (Figure 8.) Having achieved the formation of $SiCl_2$ in the Si reservoir, the reaction can then be reversed near the substrate simply by dropping the temperature to form a deposit of silicon, which may then be carburized or nitrided as the case may be. In this approach, the purpose is to cause a disproportionation of the lower chloride which is believed to result in a finer grained deposit of silicon, than would result from direct reduction of $SiCl_4$ by hydrogen. Calculations indicate that the yield of silicon by the latter reaction will not be significant at 1500°K and 40 torr with dilutions up to 20:1.

Similar considerations for reaction (5) involving trichlorosilane show that the formation of $SiCl_2$ is very energetic over the temperature range 1300°K - 1700°K, indicating that $SiHCl_3$ may be a more efficient source of $SiCl_2$.

The use of a silicon reservoir imposes an upper limit of ≈1675°K (M.P. for silicon) for the reservoir temperature since the presence of liquid Si would create handling problems in the reactor. This problem may be circumvented by using Si_3N_4 chips instead as the reducing agent, since it is more stable at these temperatures.

The reaction can then be written as:

$$SiCl_4(g) + \frac{1}{3} Si_3N_4(s) \rightleftarrows 2SiCl_2(g) + \frac{2}{3} N_2(g)$$

Figure 7 shows that reaction (8) is feasible only near 2000°K under standard conditions. Figure 8 reveals that this reaction will proceed to completion at low pressure and high dilution. Once $SiCl_2$ is formed via generation in the chip pot, thermochemical data suggest that it is relatively easy to cause disproportionation and subsequent nitridation using a suitable source. The reaction for the formation of $Si_3N_4$is:

$$3SiCl_2(g) + 4NH_3(g) \rightleftarrows Si_3N_4(s) + 6HCl(g) + 3H_2(g) \qquad (9)$$

This reaction will proceed very energetically even at room temperature. Alternatively,

$$2SiCl_2(g) \rightleftarrows Si(s) + SiCl_4(g) \qquad (10)$$

$$3Si(s) + 4NH_3(g) \rightleftarrows Si_3N_4 + 6H_2(g) \qquad (11)$$

$$3SiCl_4(g) + 4NH_3(g) \rightleftarrows Si_3N_4 + 12HCl(g) \qquad (1)$$

Calculations of standard free energy changes show that reactions (11) and (1) will both occur with nearly equal ease in the range 1500°K-1800°K.

These reactions should also occur favorably with nitrogen instead of ammonia as the nitriding specie although with much less vigor. Reactions (11) and (1) may also be carried out at much lower temperatures; however, one is then concerned with the rate of deposition and morphology of the deposit.

Several runs were made in this study as shown in Table A-4, Appendix I. Table 5 summarizes the results of evaluation of the deposits.

The deposition was carried out by passing $SiCl_4$-bearing carrier gas through the reservoir containing silicon source material (pure Si, or scrap RBSN). Several experiments were made in which the $SiCl_2$ formed in the reservoir was allowed to mix with ammonia near the substrate. In other cases, $SiCl_2$ was merely allowed to disproportionate to form silicon. In some experiments the reservoir was empty but was used as a preheat chamber for $SiCl_4$ which subsequently reacted with NH_3.

We made several runs at high chamber presures (450-600 torr) to assess the effect on deposition rate. In these runs, the nitrogen flow rates were varied from 0 to 10 liters/min. In those runs where no nitrogen was used, we did not get any deposit although argon was used as the diluent. Most of the deposits were powdery, loose and difficult to evaluate. Figure 10a shows the deposit obtained when $SiCl_4$ was passed through an empty silicon reservoir being used merely to heat the gas to about 1900°K. The deposit has a crystalline morphology with a size of about 10-15μm. The mechanical properties data suggest that the

TABLE 5 Results of tests on samples deposited in the study of silicon halide disproportionation

RUN #	kg/mm² (Load)	K_c MPa$\sqrt{m}$	TRS, MPa (ksi)	Remarks
569				White powdery deposit
573	1085 (50)			Thick powdery gray deposit
574				Grey silicon deposit under a layer of yellow powdery layer.
575	600		124 (18)	Fine crystalline Si regions of botryoidal morphology.
576				Powdery yellow deposit.
577	2645 (100)			Non uniform deposit. Partly powdery yellow, partly crystalline grey deposit.
578	1035 (100)			Grey, powdery deposit with metallic lustre.
579	3235 (100)			Non uniform deposit containing yellow powdery and grey coherent areas.
580				XRD shows αSi_3N_4 (some). Non-faceted grey crystalline surface.
581	1005 3400 (500)			Non uniform nitridation, XRD αSi_3N_4, β-SiC. Top of bar shows αSi_3N_4, βSiC and Si.
582				XRD α-SiO_2, β-Si_3N_4, some βSiC. Dark metallic rough surface with fine grained regions.
583				A mixture of grey coherent botryoidal deposit and and yellow powdery deposit.
585				XRD: α-Si_3N_4, βSi_3N_4. Mostly powdery deposit, some needle-like areas. Dissolved in Hf + HNO_3.
586				Coherent, fine grained deposit with some conical topography on the top of bar.
587				Mixture of fine and coarse globuler crystallites, columnar crystal habit.
588				XRD: αSi_3N_4, Si. Bottom-shiny grey crystals, top, grey powdery deposit.
589				XRD: Graphite, grey powdery deposit - XRD shows graphite and some Si_3N_4.
590				XRD: -Si_3N_4 + graphite. Greenish white powdery deposit.
591				Greyish white powdery deposit.
592	3380 (500)			XRD: αSi_3N_4 with traces of βSi_3N_4. White soft, fluffy deposit.
593				Mixed fine-grained and needle-like deposit.
594	3200 (500)		138 (20)	Mixture of coarse and fine faceted crystallites.
595	2930 (NC-350 3320 (Garrett SN)	4.15	138 (20)	Coarse and fine faceted grains, good adhesion to RBSN substrates.
596	2460 (500)			Coarse and fine grained crystallites.
597	2990 (500)	5.8	244 (35.4)	Fine grained deposit with poor adhesion.
598				Fine needle shaped crystals dispersed in a fine powdery deposit.
599				Fine needle shaped crystals dispersed in a fine powdery deposit.
600	2710 (500)	4.4	143 (208)	Dark, powdery surface layer on a coherent dark deposit.
601	3270 (500)	3.6		Dark faceted deposit on top, rest of deposit looks powdery.
602				Loose whisker-like crystallites on a crystalline deposit.
603				Deposit similar to run # 598 and 599.
604				Deposit similar to run # 598 and 599.
605				Mixture of fluffy whisker-like growth and a powdery deposit.
606				Black crystalline deposit and white fluffy regions. Some areas show "fused" spots.
607				No deposit.
608				No deposit.
609				No deposit.
610	1150 (100			Matrix of fine grained deposit covered with yellow powdery layer.
611	1200 (50)			Same as 610.
612	1075 (100)			Same as 610.
613				Dendritic growth near top, coarse faceted crystallites and fine grey deposit.
614				Transparent loose needle-like deposit.
615				Loose greyish whisker-like deposit.
616				Fine grained, faceted crystallites.
617	2590 (500)	3.8		Mixture of dome-like and faceted crystal morphology.
618				Smooth, amorphous looking deposit with some fine crystalline areas.

A

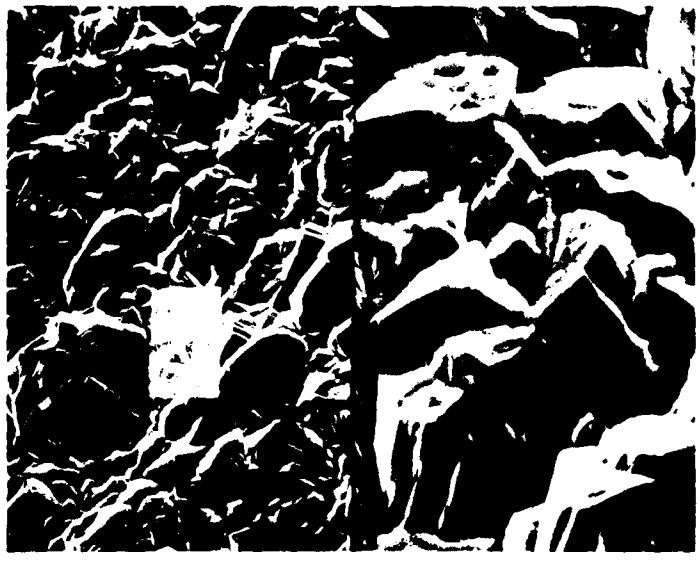

B

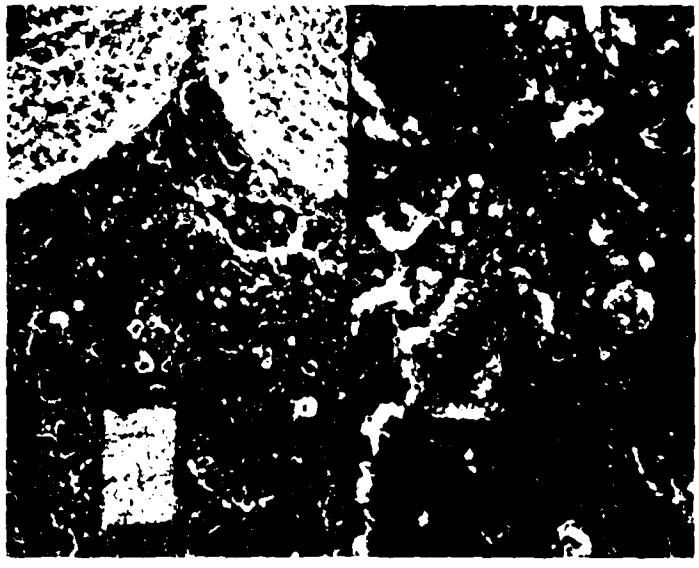

FIGURE 10 Morphology of deposit made in the silicon halide disproportionation study with $SiCl_4$.

A) 500/2500X

B) 600/3000X

material is CVD Si_3N_4 (See Table 5, run #597.) Figure 10b, on the other hand shows the structure of sample #610 which was made by passing $SiCl_4$ over CVD Si_3N_4 chips but without any ammonia. The deposit is powdery on a matrix of fine silicon layer. This and other samples that we could test showed hardness values of HV 1075 to HV 1200, suggesting that the material was probably silicon. Thus, despite the thermodynamic feasibility of nitridation of silicon,(Figure 7) we did not succeed in nitriding elemental silicon with nitrogen.

In other experiments where ammonia was used, we could form silicon nitride. In some cases traces of β-SiC were found in the XRD patterns. In one run (#589, see Table 5) where no nitrogen source was used, the deposit exhibited a β-Si_3N_4 pattern, indicating that the Si_3N_4 used as a silicon source had probably decomposed and redeposited.

In general, the results of disproportionation study were rather disappointing. The three runs made with $SiHCl_3$ instead of $SiCl_4$ resulted in a silicon nitride deposit which showed a CVD type crystal morphology. Figure 11a shows the deposit of Si_3N_4 with a crystalline morphology. Several large rounded and faceted crystallite are observed on the matrix of platelets having an average dimension of 50-100μm. Another sample, shown in Figure 11b, appears to have a rounded, botryoidal, morphology. However, it became obvious that deposition of fine grained Si_3N_4 via disproportionation of $SiCl_2$ and subsequent nitridation would be very difficult.

A

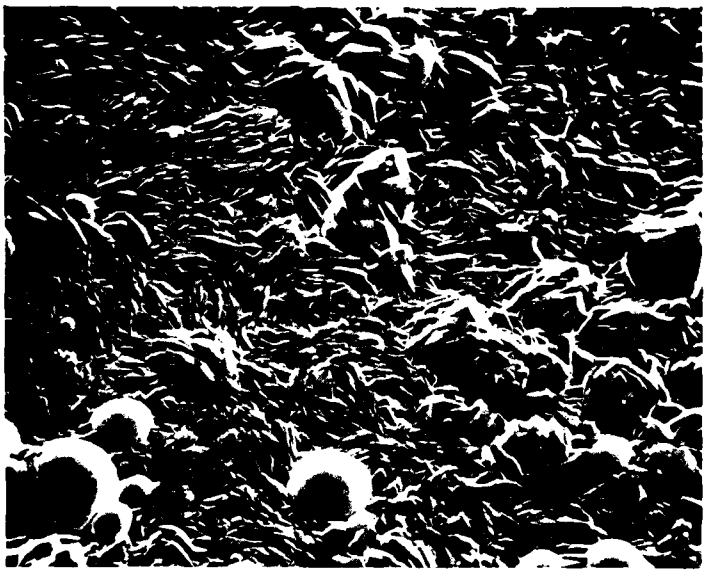

B

FIGURE 11 Morphology of deposit made in the silicon halide disproportionation study with $SiHCl_3$.

A) 70X

B) 200X/1000X

(c) "Alloying" of Si_3N_4 for grain refinement

The idea of introducing a parallel reaction in the gas stream to curtail the columnar growth of a deposit during chemical vapor deposition is not new. Researchers have effectively used this technique for example, for the grain refinement of tungsten.[17,18] In our experiments we decided to use an essentially similar approach.

During the first year on this program [1] we had examined the feasibility of using propane for this purpose. In that study, we attempted to co-deposit SiC and Si_3N_4 on the resistivety heated tungsten filaments. Although we could not succeed in doing so, we found that frequently the presence of propane in the gas stream probably led to a relatively finer, columnar crystallites. We, therefore, used this approach in an attempt to reduce the crystallite size of Si_3N_4 made in a furnace. The run conditions for these experiments are given in Appendix I, Table A-5. Table 6 summarizes the results of evaluation of deposits made with propane additions. Again, no specific trend can be detected as far as relating deposition rate with process paramenters. For example, Runs #51 and 55 were made under identical conditions but the deposition rates were different. XRD showed random orientation of deposit in one case while the other showed a strongly oriented deposit. The photomicrographs (Figure 12) showed typical, well-faceted deposits Figure 12a shows the surface topography of sample #50 (Table 6). The crystallite size is 5-10μm. By comparison, sample #56 (Figure 12b) shows massive crystals, about 30μm in size. Table 6 shows that for sample #56 the active gas concentration ($SiCl_4$ + NH_3) is much higher than for sample #50, and the deposition rate is more than doubled.

A

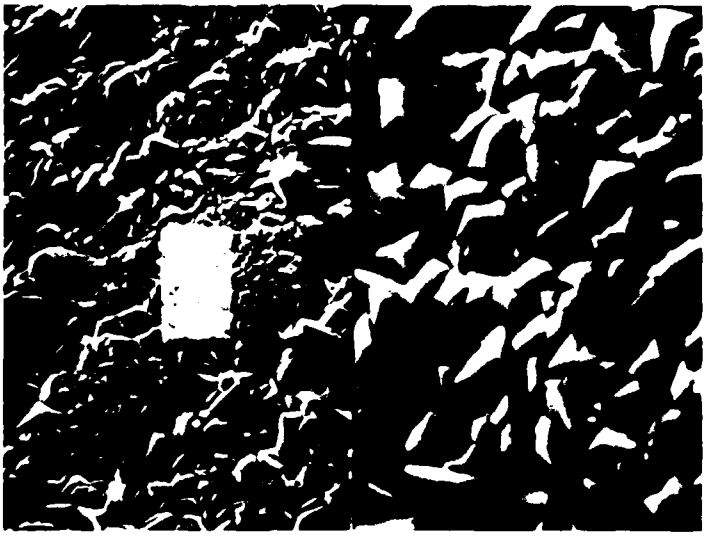

B

FIGURE 12 Morphology of Si_3N_4 made with additions of propane. to the gas stream.

A) 1000X/5000X

B) 1000X

TABLE 6 Summary of test results on Si_3N_4 made with additions of Propane

Run #	Total Pressure torr	Substrate temp °k	AGPP torr	$SiCl_4$ NH_3 ratio	C_3H_8 $SiCl_4$ ratio	PH_3 torr	Gas Velocity at T&P m/s	Depositon rate um/hr	HV kg/mm^2	K_c $MPa\sqrt{m}$	Remarks
1-50	40	1650	0.30	0.2	1.0	2.2	41.8	48	-	-	Five crystalline deposit, top appears amorphous, Strong (200) orientation) EDAX: 58.3 w/o Si.
1-50	40	1650	0.65	0.2	1.0	4.8	19.9	102	2660	2.9	Mixture of amorphous and crystalline deposits, random orientation EDAX: 59.1 w/o Si.
1-52	47	1650	4.2	1.0	1.0	33.0	1.5	42	-	-	Smooth, dull coating, (200) orientation. No SiC observed in XRD.
1-53	40	1685	5.2	0.7	1.75	43	1.7	42	-	-	Dark crystalline deposit with some large crystals *near edge*.
1-54	40	1650	2.2	2.0	1.0	33	1.4	30	-	-	Dark crystalline deposit with some botryoidal growth in the center.
1-55	40	1650	0.65	0.2	1.0	4.8	19.9	78	-	-	Coarse 30 m) crystalline deposit with dark color. Strong (210), (110) and (321) peaks. EDAX: 61.5 w/o Si, 0.2 w/o Cl.
1-56	40	1650	0.64	0.2	3.0	6.9	19.9	108	2900	3.6	Massive crystals at top, fine at bottom. XRD similar to above, but orientation after polishing changed to (222) and (004). EDAX: 60.5 w/o Si, 0.1 w/o Cl.
1-57	40	1650	0.63	0.2	6.0	10.0	19.9	66	-	-	
1-60	47	1725	0.38	0.2	3.0	26.0	15.4	168	-	-	Mixed crystal size range, clear, transparent deposit.

summarized in Table 7. The samples generally showed poor adhesion to the substrate, and strong crystal orientation, in XRD. We did not find any trace of SiC, or carbon in the deposit. The crystallite size varied considerably, as shown in Figure 13. Comparing Figures 13a and 13b an increase in the active gas concentration may have resulted in an apparent grain refinement to some extent. However, these experiments also proved to be unsuccessful in producing fine grained Si_3N_4 with any consistency.

We, therefore, decided to terminate these efforts, and attempt co-deposition of AlN. Aluminum nitride is deposited by causing a reaction between $AlCl_3$ and NH_3:

$$AlCl_3(g) + NH_3(g) \rightarrow AlN(s) + 3HCl(g) \qquad (14)$$

The study of this system was being carried out on another program sponsored by AFOSR.[7] We were conducting experiments to refine the grain structure of CVD AlN by introducing silicon in the gas stream. A natural extension of this work was to explore the feasibility of this approach in the system Si_3N_4 + Al. Some of these experiments were carried out under the AFOSR program. Since this work was directly applicable to the present program, the details of these experiments are included in this report. Table 8 gives the summary of results obtained from the samples in this work.

The sample in run #652 was made without any additions of Al and resulted in a typical CVD Si_3N_4 deposit. Two samples from this group were

A

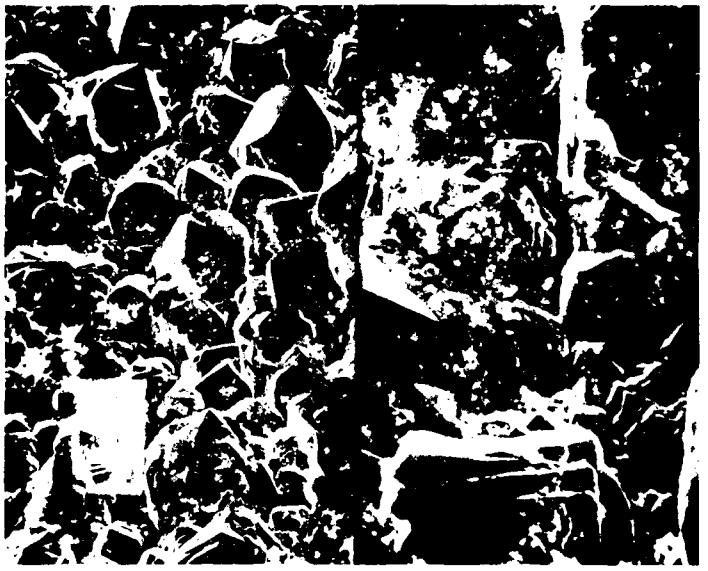

B

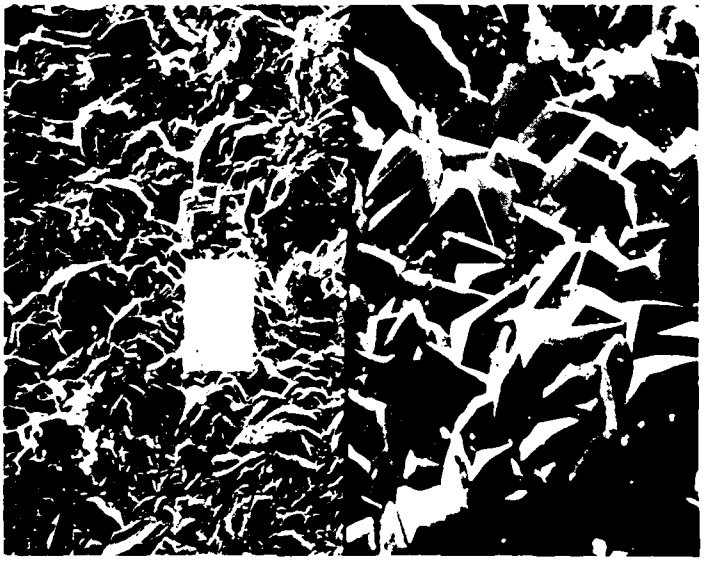

FIGURE 13 Morphology of Si_3N_4 made with methyltrichlorosilane and ammonia.

(A) AGPP = 0.61 torr 200X/1000X

(B) AGPP = 1.7 torr 200X/1000X

The higher concentration of C_3H_8 apparently only introduces greater amount of hydrogen since no carbon or SiC was detected in the XRD pattern for sample #56. The interrelationships of the various parameters in this case are interesting but unknown. Thus, in general, the addition of propane did not appear to have much beneficial effect on the grain size of the deposit.

We made another attempt to introduce a carbon source to influence the reaction between Si and N_2. Methyltrichlorosilane is an excellent precursor for the deposition of SiC. [4] The reaction is:

$$CH_3SiCl_3(g) \rightleftarrows SiC(s) + 3HCl(g) \qquad (12)$$

We attempted to influence this reaction with the addition of ammonia. We were interested in the following possible reaction, although other reactions sequences were probably also feasible.

$$CH_3SiCl_3(g) + \frac{4}{3} NH_3(g) \rightarrow \frac{1}{3}Si_3N_4(s) + HCl(g) + C(s) + 2H_2(g) \qquad (13)$$

Alternatively, it might be possible to combine reactions (12) and (13) so that co-deposition of SiC and Si_3N_4 could occur. Calculations of the change in free energy of the reactions suggested that the combined reaction would be more favorable than reaction (13) under standard conditions. If this could be achieved under reduced pressure, and other parametric constraints, we might be able to utilize the differences in the reaction rates of formation of SiC and Si_3N_4 to achieve grain refinement. The results of these experiments are

TABLE 7

Summary of test results on Si_3N_4 made with MTS as Si Source

Run #	Total Pressure Torr	Substrate Temp. °K	AGPP torr	MTS / NH_3 ratio	Pd_2 torr	Gas Velocity at T&P m/s	Deposition rate μm/hr	HV_{100} kg/mm²	K_c MPa√m	Remarks
1-46	40	1675	0.31	0.2	1.7	41.4	102	-	-	Poor adhesion, dark crystalline deposit.
1-47	40	1675	0.61	0.4	1.7	42.5	234	2930	-	Non uniform grain size, strong (20) orientation, EDAX: 59.4 w/o Si
1-48	40	1675	1.7	0.4	4.9	14.9	240	2820	3.55	Several crystallite sizes, many strong peaks but no random orientation, EDAX: 57.4 w/o Si.
1-49	40	1625	1.7	0.4	4.9	14.4	252	-	-	Non-uniform, non-adherent and partly powdery deposit. Strong (222) orientation, EDAX: 56.2 w/o Si, 0.2 w/o Cl.

TABLE 8 Summary of results on deposits made with Al as "alloying" addition

Run #	Pressure Torr	Substrate Temp. °K	Deposition Rate μm/hr	HV kg/mm² (Load)	K_c MPa$\sqrt{m}$	TRS MPa (ksi)	REMARKS
8-652	65	1600	100	3255 (100)	-	376 (55)	Non-uniform deposit morphology from top to bottom, from fine crystallites to coarse faceted crystals.
8-653	65	1625		2960 (200)	-	158 (23)	same as above.
8-654	65	1595		-	-	290 (42)	Glassy deposit with rounded domes and areas of faceted crystallites. Poor adhesion and integrity.
8-655	65	1590		3410 (100)		-	Fine grained deposit with rounded domes on the surface.
8-656	65	1590		2560 (500)	-	129 (19)	Amorphous type deposit with microcracks.
8-657	65	1585	250	2330 (500)	4.9	-	Translucent deposit with fine grained domes on the surface.
8-658	90	1595		2320 (200)	3.2	-	Dark shiny deposit with domes. Fracture surface appears glassy, non-columnar.
8-659	90	1590					Fine-grained, columnar deposit, with surface cracks.
8-660	50	1420					Whitish amber deposit on top, dark at the bottom, appears glassy in fracture.
8-661	62	1425					same as above.
16-182	73	1750	74				Fine-grained deposit, cracked near top on graphite substrates.
16-183	73	1750	-				Whisker-like growth on the entire surface.
16-184	72	1750	146				Fine grained, uniform deposit.
16-185	75	1750	174	1945	3.2	204 (29.6)	Botryoidal morphology of deposit, cracks on the surface. Size of rounded crystallites varies widely (10-50μm). Some porosity in the deposit.
16-186	75	1735					
16-187	76	1750	150				Layered deposit showing a mixture of dense columnar growth, porous banded region and preferential growth of hexagonal platelets on the surface. Generally columnar, coarse rounded crystallites. (20-50μm)
16-188	76	1750	142				
16-189	74	1750	105				
16-190	72	1750	-	2170 (300)	5.3	225 (32.6)	Faceted crystalline deposit surface with columnar grains. Surface shows randomly oriented platelets with edges nearly normal to the surface of deposit.
16-191	76	1750	194	1890	3.5	168 (24.4)	Finely cracked, botryoidal deposit with size of rounded crystallites ranging from 10 to 30μm.
16-192	79	1750	149				
16-193	91	1750	182				Layered deposit showing columnar, porous, layered and granular morphologies in the fracture cross section.

analysed extensively to study the effect of incorporation of Al. Figure 14a shows a typical CVD Si_3N_4 deposit with columnar grain structure. In comparison, the grain refinement achieved by the incorporation of Al in the material is clearly visible in Figure 14b. The distribution of Si and Al in the material is shown in the X-ray elemental density maps (Figure 15). The complimentary variation of the concentration of Al and Si is clearly visible. This suggests that both Al and Si were incorporated simultaneously since the elemental map for nitrogen showed a uniform distribution in the section. This result clearly indicated the possibility of refining the grain structure of Si_3N_4 by adding Al to the system.

Further work was carried out to select optimum deposition conditions for the incorporation of Al (Runs #182-193, Table A-7, Appendix I). In any CVD operation the compatibility of the coefficients of thermal expansion of the substrate and the coating is an important consideration. When AlN is incorporated in Si_3N_4, the value of the coefficient of thermal expansion, α, of this dual-phase coating is different from either of the constituents. This presents some problems in maintaining the integrity of the coating. We addressed this point by studying the nature of deposits on various graphite substrates and hot pressed silicon nitride bend bars.

The microscopic evaluation of the coatings revealed that although some grain refinement could be discerned, there were problems related to the deposition that were difficult to control. For example, as shown

A

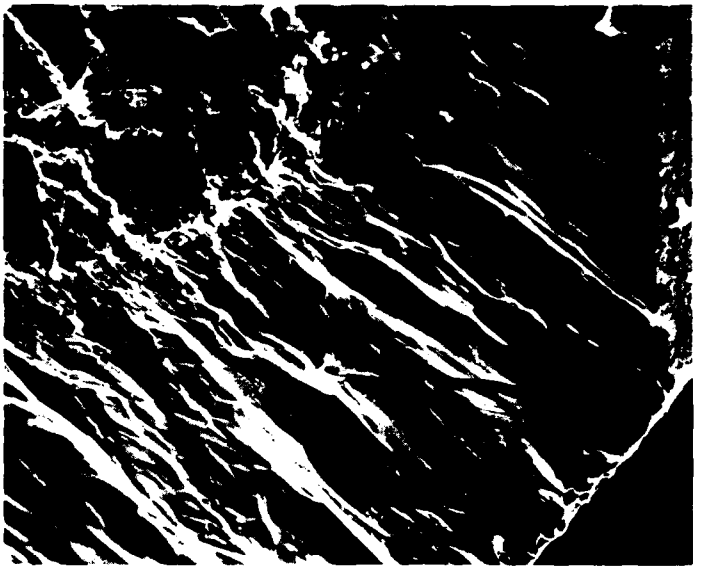

B

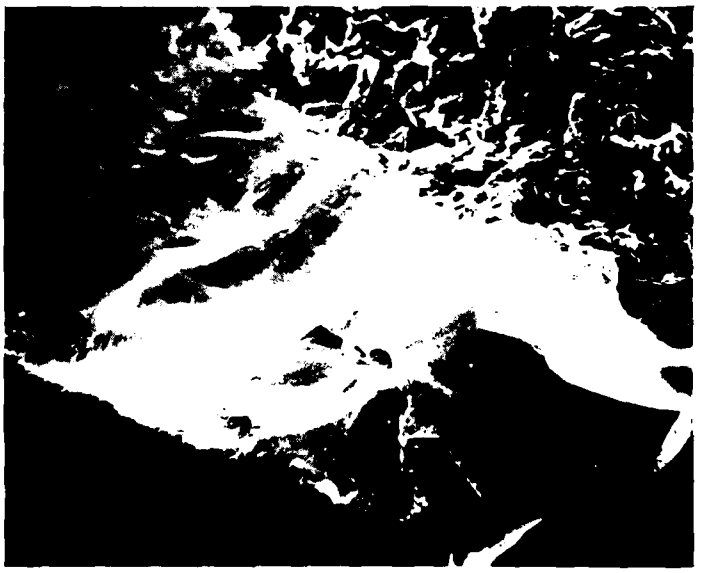

FIGURE 14 Morphology of Si_3N_4 made (A) without and (B) with Al addition

Magnification 200X

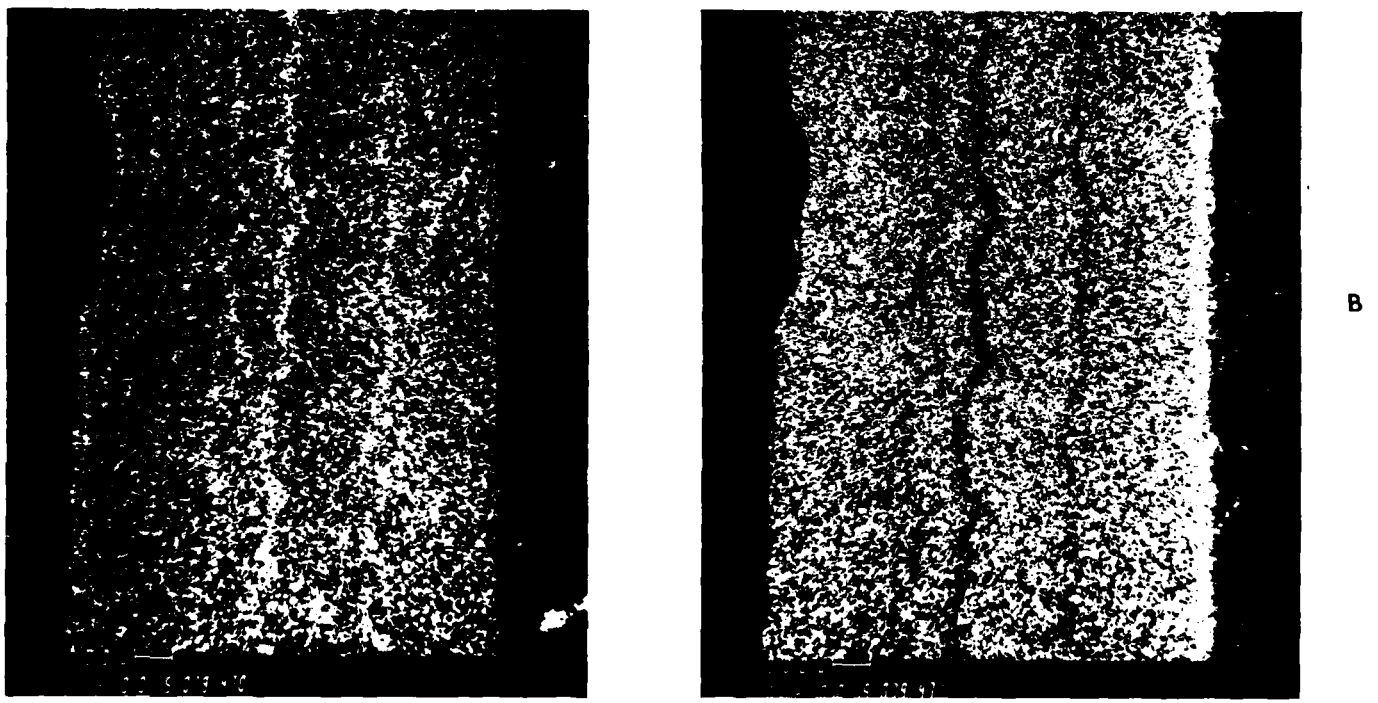

FIGURE 15 X-ray elemental density maps for the sample in Figure 14(B) showing the distribution of (A) Al and (B) Si.

in Figure 16a, we obtained a deposit which was practically free of distinct columnar grain structure although the surface revealed the uneven botryoidal topography (Figure 16b). On the other hand, another sample showed a considerable variation in the fracture topography (Figure 16c). The initial deposit was columnar, but became progressively porous. The top layer (about 10μm thick) almost totally delaminated from the rest of the coating. This layer also had an unusual crystallite orientation as revealed in Figure 16d. These variations in the morphology through the coating suggested non-uniformity of the deposition conditions during the run.

These experiments were successful to the extent that we could demonstrate the possibility of CNTD-type grain refinement in Si_3N_4 by incorporating a suitable second phase. Detailed evaluation of these samples and further exploration was not carried out due to the constraints of time and funds. However, there is no doubt that a more thorough exploration and understanding of these reactions in a systematic manner is warranted and should be continued.

(d.) Deposition of Si_3N_4 on bend bar specimens

We made a series of runs in which conventional CVD silicon nitride was made and deposited on HLM graphite and RBSN substrates. The purpose of these samples was to evaluate the CVD silicon nitride made in an indirectly heated furnace and compare the results with those obtained on tungsten filaments.[1] We tested some samples for strength, hardness, fracture toughness and crystal morphology. Some

A

B

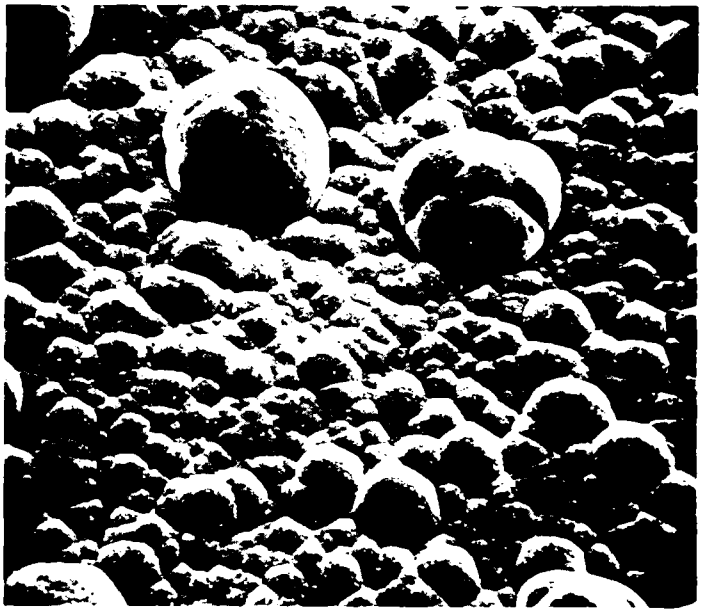

FIGURE 16 Morphology of Si_3N_4 deposited in the aluminum dopant study.

(A) 2000X

(B) 5000X

C

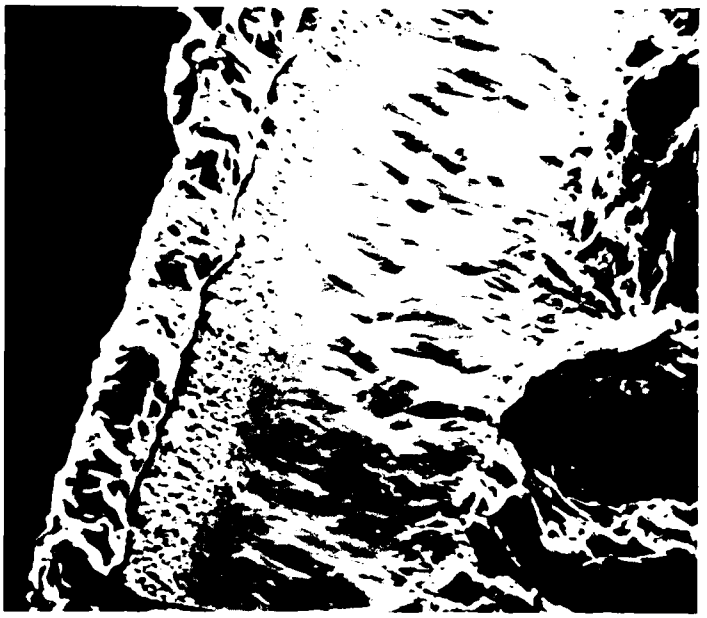

D

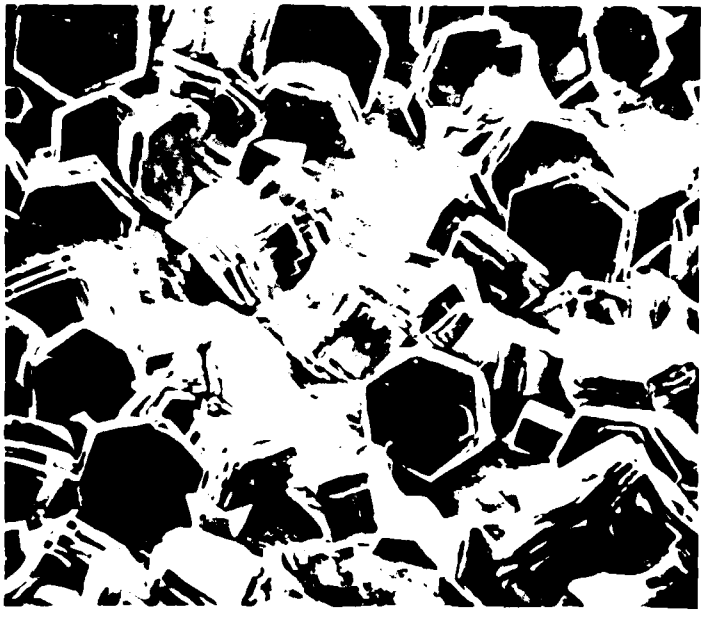

FIGURE 16 Morphology of Si_3N_4 deposited in the aluminum dopant study.

(C) 1000X

(D) 1000X

samples were sent to Mr. R. Rice of Naval Research Laboratory for evaluation. The results of our tests are summarized in Table 9. Figure 17 shows the morphology of a typical deposit in this set.

Usually, the attempts to obtain fine-grained deposits on resistance-heated filaments resulted in amorphous or glassy morphologies. The mechanical properties of samples in the present work were comparable to those in the earlier work.[1]

The fracture energy tests carried out at Naval Research Laboratory showed [19] that the CVD Si_3N_4 made at San Fernando Laboratories exhibited a fracture energy of about 20 J/m^2, comparable to values obtained on materials from other sources. The calculations of fracture energy on the basis of indentation fracture toughness measurements that we carried out gave values in the range 17 to 86 J/m^2 with an average of about 40 J/m^2. The difference probably reflects the relative sample size in the two types of tests. There is another possibility for the difference in the fracture energy values. The samples for indentation fracture toughness measurement are polished ceramographically. This procedure usually introduces a residual compressive stress on the surface. We did not anneal the samples after polishing to remove any possible residual stress. In addition, the error in the measurement of crack length using the microhardness tester at 400X probably resulted in an over-estimation of the fracture toughness by this technique of about 15%. Rice [19] also noted that the fracture strength of the samples was only about 69 MPa (10 ksi) and this was related to the large grain size of the deposit. Although we did not carry out a

TABLE 9

Summary of results on bend bar specimens

Run #	Hardness kg/mm^2 (load)	Fracture toughness K_C, $MPa\sqrt{m}$	TRS (3 point) MPa (ksi)	REMARKS
168	2505 (200)	6.1	392 (57)	HLM graphite substrate
170	2215 (500)	3.55	123 (18)	RBSN substrate
173	4130 (100)	-	197 (29)	HLM graphite substrate
175	3480 (300)	-	165 (24)	HLM graphite substrate

A

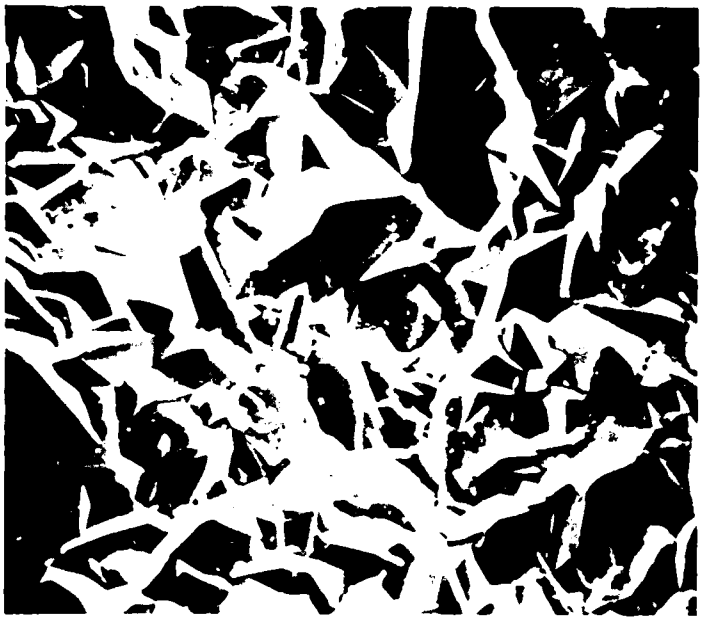

B

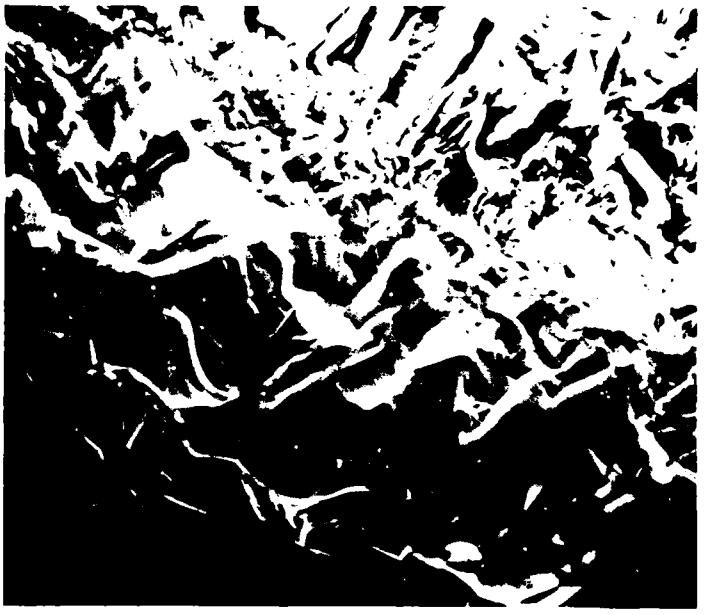

FIGURE 17 Morphology of Si_3N_4 deposit on bend bar specimens.

(A) 2000X

(B) 2000X

detailed investigation of the relationship between strength and the size of crystallites, our results generally support his findings.

(e) Measurements of electrical properties

As discussed in the experimental procedure (p. 3), this was not a part of work scope of the present program. However, the results are included here since there is an interest in Si_3N_4 as a dielectric material. The samples for these measurements were made under another program. The evaluation was carried out elsewhere. Table 10 gives data for our material. We also include data for other silicon nitrides and a SiAlON for comparison.

IV. SUMMARY AND CONCLUSIONS

The objective of the present program was to evaluate various methods of refining the grain structure of CVD Si_3N_4 deposited on an indirectly heated substrate. We examined various deposition chemistries to influence the reaction between silicon and nitrogen. Experiments were conducted to study the effects of nitrogen, argon, SiF_4, propane, MTS and aluminum on the process parameters and morphology of the deposits. We also studied the possibility of depositing elemental silicon by the disproportionation of silicon halides and its subsequent nitridation.

We found that in most chemical systems studied the tendency of $SiCl_4$ (or SiF_4) to form intermediate species in the vapor phase by reacting with NH_3 caused difficulties in controlling the process parameters. This reaction resulted in deposits having a variety of crystal morphologies and properties. However, the simultaneous presence of aluminum chloride and its reaction with ammonia resulted in a non-columnar deposit of Si_3N_4-AlN. Thus, although the attempts to apply the CNTD process for depositing non-columnar, fine-grained Si_3N_4 were largely unsuccessful, valuable understanding was gained regarding the chemistry of Si_3N_4 deposition. The salient points were:

(A) The silicon halide-ammonia system is not amenable to CNTD-type grain refinement due to the propensity for vapor phase reaction and formation of non-volatile intermediates.

(B) Additions of carbon, either as MTS or as propane, do not cause grain refinement in Si_3N_4 under the experimental conditions used in the present work.

(C) The codeposition of AlN with Si_3N_4 apparently permits grain refinement. This is probably due to the competitive nature of nitridation reactions for Al and Si. A non-columnar deposit of AlN-Si_3N_4 is obtained.

The mechanical properties of Si_3N_4 made by the indirect heating of substrates were comparable to those obtained on directly heated substrates. The flexure strength values were 205 MPa (29.8 ksi) ± 80 MPa (11.6 ksi), with values as high as 450 MPa (65 ksi). The hardness of the deposits was usually in the range HV 2500 to HV 3000, with values as high as HV 4130 and as low as HV 1900. The indentation fracture toughness was about 4.0 MPa$\sqrt{m}$, with values as high as 5.8 MPa$\sqrt{m}$.

In conclusion, the present work clearly demonstrated the potential of vapor deposited silicon nitride in terms of achievable properties. The concept of codeposition of a second phase to minimize or eliminate the columnar growth habit was shown to be feasible in the initial experiments.

An advantage of the vapor deposition technique is the possibility of studying very pure alloy systems. Conventional powder technology is very often limited by the presence of impurities, intentional or otherwise. Therefore, it should be noted that the vapor deposition technology offers the possibility of studying Si-Al-N system without having to deal with oxygen. The initial success of the codeposition work warrants further development work to refine the system and study the feasibility of depositing a range of Si_3N_4-AlN compositions for high temperature applications.

TABLE 10 Dielectric Properties of Si_3N_4 at room temperature

MATERIAL	FREQUENCY $x10^9$Hz	ε'	TANδ
CVD Si_3N_4 (SFL)	9.375	7.04	7.5×10^{-3}
HPSN[20]	9.3	3.2	1×10^{-2}
HPSN + 5% MgO[20]	9.3	5.65	4×10^{-3}
Z≈4 SIALON (HP)[20]	9.3	5.1	3.7×10^{-2}
RBSN[21]	8-10	5.6	2×10^{-3}

REFERENCES

1. Holzl, R.A.:"Investigation of the CNTD Mechanism and Its Effect on Microstructure and Properties of Silicon nitride," Summary Report, U.S. Naval Air Systems Command Contract #N00019-77-C-0395. July, 1979.

2. Evans, A.G. and Charles, E.A.: J. Amer. Ceram. Soc., 57, 371 (1976).

3. Holzl, R.A.:"Grain Refinement by Thermochemical Means," Proceedings of 6th International Conference on Chemical Vapor Deposition, Atlanta, Georgia, The Electrochemical Society, Princeton, N.J., (1977), p. 107.

4. Holzl, R.A.:"An Investigation of the CNTD Mechanism and Its Effect on Microstructural Properties," U.S. Air Force Office of Scientific Research Contract #F49620-77-0086, March, 1977.

5. Stiglich, J.J., Bhat, D.G., and Holzl, R.A.: Ceramurgia International, 6 (1), 3 (1980).

6. Dutta, S., Rice, R.W., Graham, H.C. and Mendiratta, M.G.: "Characterization and Properties of Controlled Nucleation Thermochemical Deposited (CNTD) Silicon Carbide," NASA Tech. Memo 79277, paper presented at 80th Annual Meeting of American Ceramic Society, Detroit, Michigan, May, 1978.

7. Panos, R.M. and Bhat, D.G.: "An Investigation of the CNTD Mechanism and Its Effect on Microstructural Properties." Interim Report, U.S. Air Force Office of Scientific Research, Contract #F49620-79-C-0041, March, 1980.

8. Gazzara, C.P. and Reed, D.: "A Computed X-ray Diffraction Powder Pattern for Alpha and Beta Silicon Nitride," AMMRC TN 75-4, Army Materials and Mechanics Research Center, Watertown, Mass., April 1975.

9. Kijima, K., Setaka, N. and Tanaka, H.: J. Cryst. Growth, 24/25, 183 (1974).

10. JANAF Thermochemical Tables, Second Edition June 1971.

11. Nihara, K. and Hirai, T.: J. Mater. Sci., 12, 1243 (1977)

12. Wannagat, U.: "Advances in Inorganic Chemistry and Radiochemistry, Vol. 6, p. 225, Academic Press, New York (1964)

13. Lin, S. - S.: J. Electrochem. Soc., 125, 1877 (1978).

14. Lin, S. - S.: J. Electrochem. Soc., 124, 1954 (1977).

15. Rochow, E. G.: "The Chemistry of Silicon," Pergamon Texts in Inorganic Chemistry, vol. 9, p. 1340, Pergamon Press, New York (1973).

16. Holzl, R.A.: Unpublished work.

17. Seymore, W.C. and Byrne, J.G.: "The Influence of $MoCl_5$ on the Chemical Vapor Deposition of Tungsten from WF_6," Proceedings of 5th International Conference on Chemical Vapor Deposition, England, p. 815 (1975)

18. Landingham, R.L. and Austin J.H.: J. Less Common Metals, 18 229 (1969)

19. Rice, R.: Private Communication.

20. Thorp, J.S. and Sharif, R.I., J. Mater. Sci., 12, 2274 (1977)

21. Walton, J.D.: Amer. Ceram. Soc. Bull., 53, 255 (1974)

22. Popov, E.P.: "Introduction to Mechanics of Solids," p. 202, Prentice-Hall, Inc. Englewood Cliffs, N.J. (1968).

APPENDIX I: Deposition Conditions for Si_3N_4

TABLE A-1 Deposition conditions for Si_3N_4 made with nitrogen as carrier gas for the precursors

Run #	Gas Flow Rate, ml/min $SiCl_4$	NH_3	H_2	N_2	Total Pressure Torr.	Substrate Temp. °K	Run Time min	Deposition rate μm/hr
1-1	30	150	400	2700	25	1635	30	78
1-2	30	150	400	2700	25	1575	30	78
1-3	30	150	400	2700	25	1500	30	-
1-4	30	150	400	1000	25	1500	30	-
1-5	30	150	400	4300	26	1650	30	48
1-6	30	150	400	8600	39	1650	30	48
1-7	30	150	400	11,550	52	1650	30	48
1-8	30	150	400	11,750	52	1650	120	66
1-9	30	150	400	11,750	48	1620	60	48
1-10	30	150	400	15,000	64	1650	60	36
1-11	30	150	400	15,000	60	1675	60	18
1-12	30	150	400	15,000	66	1735	90	60
1-13	30	150	400	2700	25	1635	180	66
1-14	30	150	400	8600	40	1650	180	102
1-15	30	150	400	11,550	52	1700	30	96
1-16	30	150	400	11,550	55	1650	30	24
1-17	30	150	400	11,550	62	1650	45	54
1-18	30	150	400	11,550	61	1700	45	36
1-19	30	150	400	11,550	58	1750	60	72
1-20	30	150	400	11,550	58	1800	60	-
1-21	30	150	400	11,550	59	1650	30	-
1-22	30	150	400	8600	45	1650	60	66
1-23	30	150	400	8600	47	1650	60	-
1-24	60	300	800	15,865	78	1650	30	150
1-25	37.5	187.5	500	8600	48	1650	60	-
1-29	250	87	975	2400	28	1525	120	-
1-35	30	150	400	8200	41	1645	90	48
1-36	30	150	400	8200	40	1645	90	-
1-37	30	150	1400	7200	42	1645	60	90
1-38	30	150	400	4100	40	1645	90	60
1-58	30	140	4400	3720	47	1650	60	36
1-59	30	150	4400	3720	47	1775	60	180

TABLE A-2: Deposition conditions for Si_3N_4 made with argon as the diluent gas

Run #	Gas Flow rate, ml/min. $SiCl_4$	NH_3	H_2	Ar	Total Pressure Torr.	Substrate Temp. °K	Run Time min.	Deposition rate μm/hr
1-26	275	85	975	2400	28	1525	30	204
1-27	275	150	975	2400	25	1525	120	126
1-28	275	75	975	2400	25	1520	120	-
1-30	275	85	975	2400	28	1525	60	-
1-31	275	85	975	2400	28	1475	30	-
1-32	275	100	975	2400	28	1475	30	360
1-33	275	100	975	2400	28	1475	90	156
1-34	275	100	975	2400	28	1425	90	102
1-39	60	300	800	15,865	67	1650	60	126
1-40	60	300	800	15,865	67	1645	180	126
1-41	275	100	975	2400	29	1645	30	300
1-42	275	100	975	2400	29	1545	30	-
1-43	275	100	975	4800	28	1525	30	186
1-44	275	100	975	4800	28	1535	120	-
1-45	275	100	975	10,800	50	1625	60	102

TABLE A-3 Deposition conditions for experiments using SiF_4 as silicon source*

Run #	Gas Composition, ml/min					Total Pressure Torr.	Gas Temp. °K	Substrate Temp. °K	Run Time Min.	Deposition Rate Å/hr.
	SiF_4	NH_3	Ar	H_2	N_2					
16-78	54	410	500	3877	2913	40	650	1775	30	245
16-79	54	410	500	3877	2913	40	605	1725	30	169
16-80	54	410	500	3877	2913	40	725	1725	60	178
16-81	100	410	500	3877	2913	40	745	1775	60	216
16-82	100	410	500	3877	2913	60	575	1775	60	237
16-83	150	410	500	3877	2913	80	570	1775	60	229
16-84	200	410	500	3877	2913	40	615	1775	60	195
16-85+	200	410	500	3877	2913	40	700	1875	5	-
16-86	200	410	500	7760	6650	80	550	1875	60	288
16-87	400	820	500	7760	6650	80	645	1875	30	245
16-88	400	820	500	7760	6650	80	690	1875	60	474
16-89	400	820	500	9200	6650	80	695	1875	60	372

*Substrate used in all experiments was HLM graphite except last two runs where RBSN was used.

+Experiment stopped due to vacuum system failure.

TABLE: A-4 Deposition conditions for the study of disproportionation of silicon halide

RUN #	Gas Flow Rate, ml/min $SiCl_4$	NH_3	H_2	N_2	Ar	$SiHCl_3$	Total Pressure Torr	Si Reservoir Temp. °K	Substrate Temp. °K	Run Time Min	Substrate Materials used
8-569	500	0	0	0	1000	0	41	1975	1425	10	UT-22 graphite
8-573	275	0	0	0	2000	0	279	1950	1115	15	UT-22 graphite
8-574	200	70	0	0	2000	0	292	1925	1300	30	UT-22 graphite
8-575	200	100	125	0	2000	0	53	1975	1185	30	UT-22 graphite
8-576	200	200	125	0	2000	0	58	1975	1275	30	UT-22 graphite
8-577	200	200	125	0	2000	0	60	1975	1425	30	graphite 1/4" dia. rod
8-578	200	0	125	2000	0	0	60	1975		30	graphite 1/4" dia. rod
8-579	100	200	125	2000	0	0	55	1975	1435	45	
8-580	100	200	0	2200	0	0	55	1975	1540	60	UT-22 graphite
8-581	100	200	0	2200	0	0	57	1975		60	UT-22 graphite
8-582	100	1000	0	2200	0	0	50	1975			UT-22 graphite
8-583	100	1000	0	2200	0	0	55	1675	1475	30	UT-22 graphite
8-585	100	500	250	2000	0	0	32	1975	1575	30	UT-22 graphite
8-586	100	500	0	2200	0	0	37	1995	1875	15	UT-22 graphite
8-587	100	500	250	2200	0	0	45	1775	1725	60	UT-22 graphite
8-588	200	0	0	2200	0	0	44	1975	1650	60	UT-22 graphite
8-589	500	0	0	0	1100	0	50	1925	1525	50	UT-22 graphite
8-590	500	0	0	0	1200	0	40	1975	1525	30	UT-22 graphite
8-591	100	0	0	2200	0	0	45	1900	1625	20	UT-22 graphite
8-592	100	500	0	2200	0	0	45	1800	1625	60	UT-22 graphite
8-593	100	500	0	2200	0	0	47	1500	1820	30	UT-22 graphite
8-594	100	500	0	2200	0	0	45	-	1815	60	NC-350 (Airesearch)RBSN
8-595	100	500	0	2200	0	0	43	-	1800	60	NC-350 (Airesearch)RBSN
8-596	100	500	0	2200	0	0	45	-	1775	30	NC-350 (Airesearch)RBSN
8-597	100	500	0	2200	0	0	45	-	1780	15	UT-22,Navair RBSN
8-598	100	500	0	2200	0	0	46	1925	1810	30	NC-350, graphite
8-599	300	500	0	2200	0	0	45	1910	1810	15	NC-350, graphite
8-600	300	2100	0	2200	0	0	50	1910	1810	30	NC-350, graphite
8-601	300	1500	0	2200	0	0	52	1900	1800	30	NC-350, graphite
8-602	300	1500	0	2200	0	0	50	1925	1825	30	NC-350, graphite
8-603	100	0	200	400	0	0	584	1900	1700	30	NC-350, graphite
8-604	100	0	200	400	0	0	584	1925	1700	60	NC-350, graphite
8-605	100	0	600	400	0	0	590	1875	1675	30	graphite
8-606	200	0	1200	400	0	0	597	1925	1700	25	graphite
8-607	500	0	475-4500	0	1000	0	470	-	1520	40	graphite
8-608	500	0	1400	0	1000	0	470	-	1675	15	graphite
8-609	500	0	10,000	0	1000	0	483	-	1675	40	graphite
8-610	500	0	10,000	1500	0	0	483	-	1700	30	graphite
8-611	500	0	10,000	1600	0	0	483	-	1700	30	graphite
8-612	500	0	10,000	5000	0	0	483	-	1710	30	graphite
8-613	500	100	10,000	5000	0	0	483	-	1710	30	
8-614	500	0	2000	10,000	0	0	483	-	1875	30	graphite 1/4"dia. rod
8-615	500	0	10,000	9000	0	0	457	-	1695	187	UT-22, NC350(AMMRC) 7 min. Si deposition, 3 hr. nitriding at 16000 ml/min N_2 flow
8-616	0	0-1000	0	5000	0	500	50	1550	1625	35	UT-22 graphite
8-617	0	200	0	5000	0	500	40	1525	1655	45	UT-22 graphite
8-618	0	200	0	7000	0	500	50	1475	1650-1525	20	UT-22 graphite

NOTES (1) The first 12 runs up to 8-583 were conducted under AFOSR grant within the scope of a similar investigation in the SiC deposition.

(2) In all runs except the last 3 (i.e. #616, 617, 618), Si_3N_4 scrap was used in the reservoir.

TABLE A-5: Deposition conditions for Si_3N_4 made with additions of propane

Run #	Gas Flow rate, ml/min					Total Pressure Torr.	Substrate Temp. °K	Run Time min	Deposition Rate µm/hr
	$SiCl_4$	NH_3	H_2	N_2	C_3H_8				
1-50	30	150	400	8600	30	40	1650	30	48
1-51	30	150	400	3720	30	40	1650	30	102
1-52	25	26	220	94	26	47	1650	30	42
1-53	25	35	220	48	44	40	1685	60	42
1-54	25	12	140	94	26	40	1650	60	30
1-55	30	150	400	3720	30	40	1650	90	78
1-56	30	150	400	3720	90	40	1650	90	108
1-57	30	150	400	3720	180	40	1650	60	66
1-60	30	150	4400	3720	90	47	1775	60	168

TABLE A-6: Deposition conditions for Si_3N_4 using methyltrichlorosilane (MTS) as Si source

Run #	Gas Flow rate, ml/min				Total Pressure Torr	Substrate Temp. ^{o}K	Run Time min	Deposition Rate μm/hr
	MTS	NH_3	H_2	N_2				
1-46	30	150	400	8600	40	1675	30	102
1-47	60	150	400	8600	40	1675	30	234
1-48	60	150	400	2680	40	1675	30	240
1-49	60	150	400	2680	40	1625	30	252

TABLE A-7 Deposition Conditions for Si_3N_4 "alloyed" with Aluminum

Run No.	$SiCl_4$	NH_3	H_2	N_2	Ar	HCl	Total Pressure Torr	Gas Temp. °K	Substrate Temp. °K	Run Time Min.	Deposition Rate μm/hr
16-182	270	540	8180	38,380	-	303	73	1120	1750	30	37
16-183	270	540	8180	38,380	-	303	73	1155	1750	60	-
16-184	270	540	8180	38,380	-	-	72	1105	1750	30	73
16-185	270	540	8240	38,380	-	303	75	1135	1750	30	87
16-186	270	540	8240	38,380	-	303	75	1190	1750	60	-
16-187	270	540	8240	38,380	200	303	76	1210	1750	30	75
16-188	270	540	8240	38,380	200	152	76	1065	1750	30	71
16-189	270	540	8240	38,380	200	76	74	1055	1750	60	105
16-190	270	540	8240	38,380	200	50	72	1055	1750	60	-
16-191	270	540	8240	38,380	200	404	76	1035	1750	35	113
16-192	270	540	8240	38,380	200	404	79	1020	1750	60	149
16-193	270	540	12,618	38,380	200	404	91	985	1750	35	106

TABLE A-5: Deposition conditions for bend bar specimens

Run #	Gas Flow rate, ml/min				Total Press. Torr*	Gas Temp. °K	Substrate Temp. °K	Run Time Min	Substrate Material
	$SiCl_4$	NH_3	H	N					
16-168	270	540	8240	38,380	72	990	1750± 5	25	HLM graphite ben[illegible]
16-169	270	540	8240	38,380	80	920	1750± 5	25	RBSN bend bar
16-170	270	540	8240	38,380	80	1095	175[illegible]	25	HLM graphite, and RBSN bend bars
16-171	270	540	8240	38,380	86	1166	1750± 5	25	HLM graphite, and RBSN bend bars
16-172	270	540	8240	15,720	73	1100	1750± 5	25	HLM graphite, and RBSN bend bars
16-173	270	540	8240	38,380	83	1070	1750± 5	25	HLM graphite, and RBSN bend bars
16-174	270	540	8240	38,380	73	1100	1750± 5	25	HLM graphite, and RBSN bend bars
16-175	270	540	8240	38,380	78	1095	1750± 5	30	HLM graphite, and RBSN bend bars
16-176	270	540	8240	38,380	78	1100	1750± 5	30	HLM graphite, and RBSN bend bars
16-177	270	540	8240	38,380	74	1095	1750± 5	25	HLM graphite, and RBSN bend bars
16-178	270	540	8240	38,380	72	-	1750± 5	25	HLM graphite bend bar
16-179	270	540	8240	38,380	76	-	1750± 5	25	HLM graphite bend bar
16-180	270	540	8240	38,380	80	-	1750± 5	25	HLM graphite bend bar
16-181	270	540	8240	38,380	72	-	1750± 5	25	HLM graphite bend bar

*[illegible] pressures [illegible] These values do not represent any conscious effort to change [illegible] but taken to show [illegible] within the experimental [illegible]

APPENDIX II: Calculation of transverse rupture strength of a coated beam

The calculation of the transverse rupture strength of a simple beam is accomplished by means of the flexure formula. When the beam is composed of different materials, having different elastic moduli, the calculations can be made by mathematically converting the composite beam to that made of any of the constituent materials comprising the original beam. Thus, when it is of interest to determine the strength of the coating of material A on a bar of material B, the composite beam is converted to a beam of material A by the method of equivalent sections.[22] In this method the cross section of the substrate (B) is replaced by an equivalent section of the coating such that at a given magnitude of axial strain, the forces developed in the substrate and the equivalent section of the coating are equal. Then the entire section can be treated as a single homogeneous material. The equivalent section is generated by changing the dimension of the substrate in the direction parallel to the neutral plane.

For a given axial strain e, the force developed on the substrate is $F_s = e.E_s.A_s$. At the same point in the coating, the force is $F_c = e.E_c.A_c$. For $F_s = F_c$, we have $E_c.A_c = E_s.A_s = nE_cA_s$ where $n = E_s/E_c$. Thus the area of cross section of the coating to replace an equivalent area of the substrate is $n.A_s$.

For a bend bar of rectangular cross section as shown in Figure A-1 the area of the substrate ($A_s = b_s.h_s$) is transformed into an equivalent area of the coating by changing b_s to $n.b_s$. Then, the moment of inertia

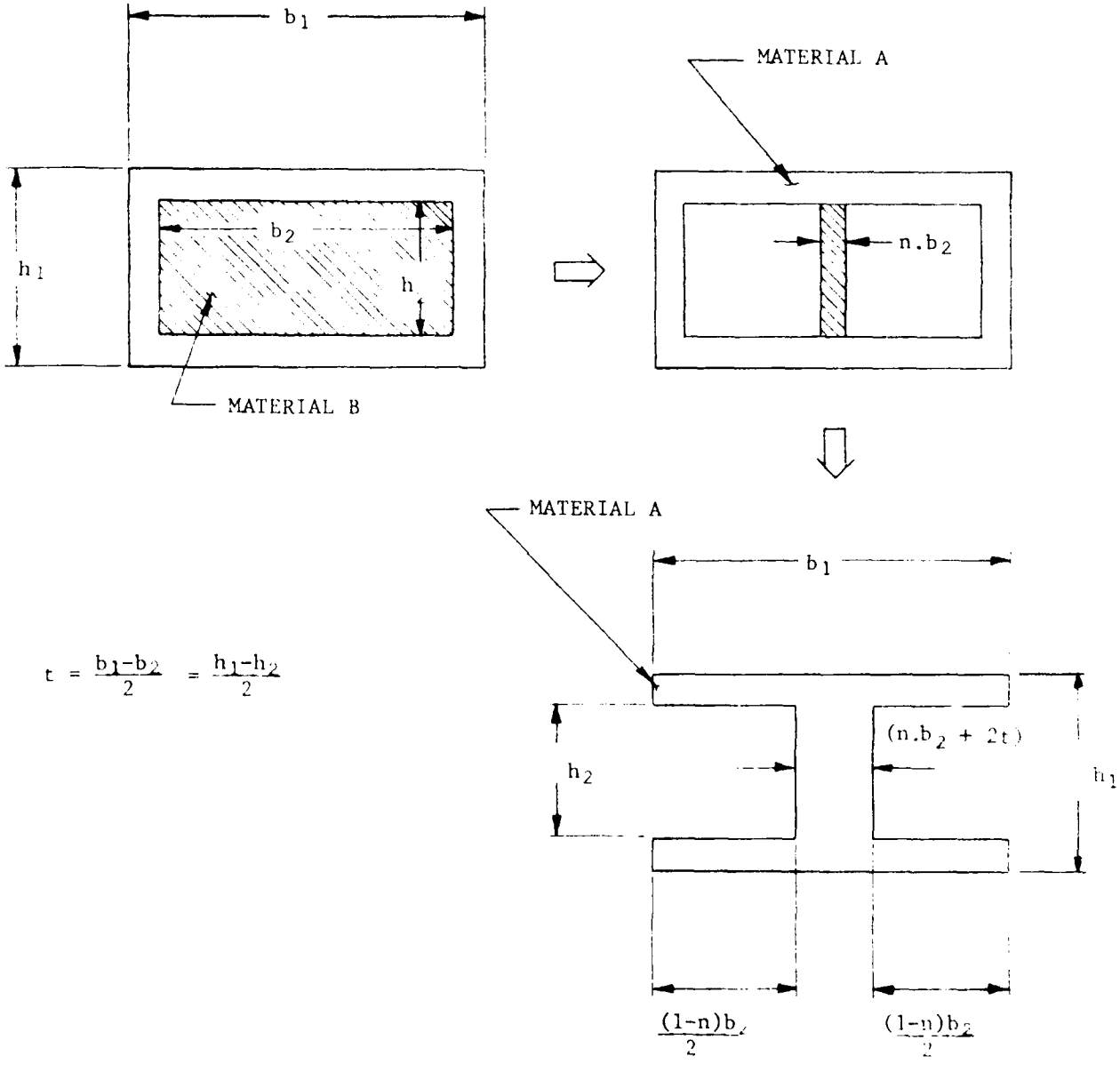

$$t = \frac{b_1 - b_2}{2} = \frac{h_1 - h_2}{2}$$

FIGURE A-1 METHOD OF EQUIVALENT SECTION

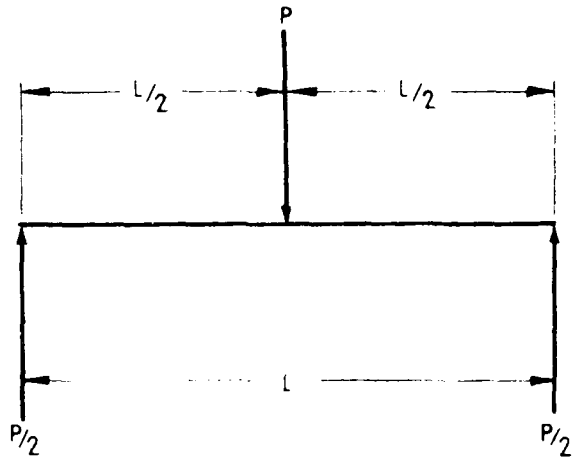

(a) 3-point flexure

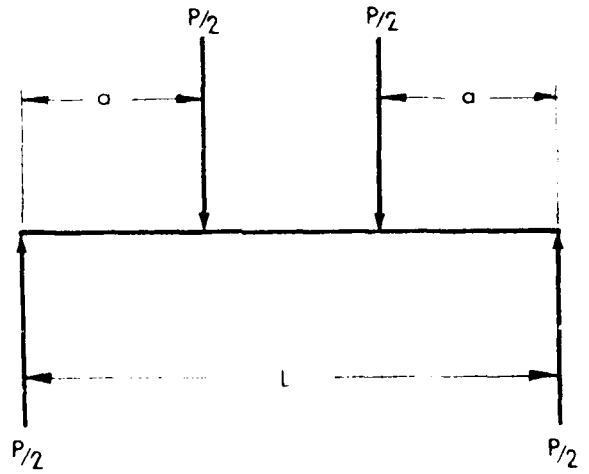

(b) 4-point flexure

Fig. A 2 Loading configurations in flexure tests

of the equivalent cross section which becomes an "I" beam, is given by

$$I = \frac{b_1 h_1^3 - (1-n)\, b_2 h_2^3}{12}$$

Then, for a three point flexure (center-point loading) test (Figure A-2)

$$TRS = \frac{3P\ell h_1}{2\{b_1 h_1^3 - (1-n)\, b_2 h_2^3\}}$$

It is assumed in the above equation that the failure occurs in the center of the span. When the failure occurs elsewhere, the flexure formula is modified to

$$TRS = \frac{3Ph_1 (1 - 2x)}{2\{b_1 h_1^3 - (1-n)\, b_2 h_2^3\}}$$

Where x is the distance between the central loading pin and the point of fracture. The expression for the four-point flexure test is

$$TRS\ (4\text{-point}) = \frac{3\ Pah_1}{b_1 h_1^3 - (1-n)\, b_2 h_2^3}$$

where a can be $\ell/3$ (1/3 - four point) or $\ell/4$ (1/4 - four point), as shown in Figure A-2.

DISTRIBUTION LIST

	No. of Copies
Naval Air Systems Command Washington, D.C. 20361 Attention: AIR 00D4 12 310C 1 320A 1 5163D4 25	39
Office of Naval Research Washington, D.C. 20360 Attention: Code 471	1
White Oak Laboratory Naval Surface Weapons Center White Oak, Maryland 20910 Attention: Code 2301	1
Naval Research Laboratory Washington, D.C. 20390 Attention: Code 6360	1
David W. Taylor Naval Ship Research & Development Center Annapolis, Maryland 21402 Attention: W. Smith, Code 2832	1
Naval Air Propulsion Center Trenton, New Jersey 08638 Attention: R. Valori, Code PE 72	1
Naval Undersea Center San Diego, California 92132 Attention: Dr. J. Stachiw	1
Naval Air Development Center Materials Application Branch, Code 6061 Warminster, Pennsylvania 18974	1
Air Force Wright Aeronautical Laboratories Wright-Patterson, Air Force Base Dayton, OH 45433 Attention: Dr. J. Dill POSL 1 Dr. H. Graham MLLM 1 Mr. B.D. McConnell MLBT 1 Ms. K. Lark MLTM 1	4
Brookhaven National Laboratory Upton, N.Y. 11973 Attention: Dr. D. Van Rooyen	1

No. of Copies

Director
Applied Technology Laboratory 1
U.S. Army Research & Technology Laboratories
Fort Eustis, Virginia 23604
Attntion: DAVDL-ATL-ATP (Mr. Pauze)

U.S. Army Research Office 1
Box CM, Duke Station
Durham, North Carolina 27706
Attention: CRDARD

U.S. Army MERDC 1
Fort Belvoir, Virginia 22060
Attention: W. McGovern (SMEFB-EP

Army Materials and Mechanics Research Center 1
Watertown, Massachusetts 02172
Attention: Dr. R.N. Katz

NASA Headquarters 1
Washington, D.C. 20546
Attention: J.J. Gangler, RRM

NASA Lewis Research Center 2
21000 Brookpark Road
Cleveland, Ohio 44135
Attention: Dr. E. Zaretsky 1
W. A. Sanders (49-1)
and Dr. T. Hergell

Defense Advanced Research Project Office 2
1400 Weilson Boulevard
Arlington, Virginia 22209
Attention: Dr. Van Reuth 1
Dr. Buckley 1

Inorganic Materials Division 1
Institute for Materials Research
National Bureau of Standards
Washington, D.C. 20234

University of California 1
Lawrence Berkeley Laboratory
Hearsy Mining Building
Berkeley, California 94720
Attention: Dr. L. Froschauer

	No. of Copies
Department of Engineering University of California Los Angeles, California 90024 Attention: Profs. J.W. Knapp and G. Sines	1
Department of Metallurgy Case-Western Reserve University Cleveland, Ohio 44106 Attention: Dr. A. Heuer	1
Engineering Experiment Station Georgia Institute of Technology Atlanta, Georgia 30332 Attention: J.D. Walton	1
Department of Engineering Research North Carolina State University Raleigh, North Carolina 27606 Attention: Dr. H. Palmour	1
Materials Research Laboratory Pennsylvania State University University Park, Pennsylvania 16802 Attention: Prof. Rustum Roy	1
Rensselaer Polytechnic Institute 110 Eighth Street Troy, New York 12181 Attention: R.J. Diefendorf	1
School of Ceramics Rutgers, The State University New Brunswick, New Jersey 08903	1
Virginia Polytechnic Institute Minerals Engineering Blacksburg, Virginia 24060 Attention: Dr. D.P. H. Hasselman	1
Aerospace Corporation Materials Laboratory P.O. Box 95085 Los Angeles, California 90045	1
Supervisor, Materials Engineering Department 93-39M AiResearch Manufacturing Company of Arizona 402 South 36th Street Phoenix, Arizona 85034	1

	No. of Copies
Materials Development Center AVCO System Division Wilmington, Massachusetts 01887 Attention: Tom Vasilos	1
Battelle Memorial Institute Ceramics Department 505 King Avenue Columbus, Ohio 43201	1
Metals and Ceramics Information Center Battelle Memorial Institute 505 King Avenue Columbus, Ohio 43201	1
Research and Development Division Carborundum Company Niagara Falls, New York 14302 Attention: Mr. C. McMurty	1
Ceramic Finishing Company Box 498 State College, Pennsylvania 16801	1
Ceradyne, Inc. Box 1103 Santa Ana, California 92705	1
Coors Porcelain Company 600 Ninth Street Golden, Colorado 80401 Attention: Research Department	1
Federal-Mogul Corporation Anti-Friction Bearing R&D Center 3980 Research Park Drive Ann Arbor, Michigan 48104 Attention: D. Glover	1
Metallurgy and Ceramics Research Department General Electric R&D Laboratories P.O. Box 8 Schenectady, New York 12301	1
Space Sciences Laboratory General Electric Company P.O. Box 8555 Philadelphia, Pennsylvania 19101	1

	No. of Copies
Hughes Aircraft Company Culver City, California 90230 Attention: Mr. M.N. Gardos	1
IIT Research Institute 10 West 35th Street Chicago, Illinois 60616 Attention: Ceramics Division	1
Industrial Tectonics, Inc. 18301 Santa Fe Avenue Compton, California 90224 Attention: Hans R. Signer	1
Kaweki-Berylco Industry Box 1462 Reading, Pennsylvania 19603 Attention: Mr. R.J. Longnecker	1
Research and Development Division Arthur D. Little Company Acorn Park Cambridge, Massachusetts 02140	1
Mechanical Technology, Inc. 968 Albany-Shaker Road Latham, New York 12110 Attention: Dr. E.F. Finkin	1
North American Rockwell Sicence Center P.O. Box 1085 Thousand Oaks, California 91360	1
Norton Company Industrial Ceramics Division One New Bond Street Worcester, Massachusetts 01606 Attention: Dr. M. Torti	1
Ceramic Division Sandia Corporation Albuquerque, New Mexico 87101	1
Engineering and Research Center SKF Industries, Inc. 1100 First Avenue King of Prussia, Pennsylvania 19400 Attention: L. Sibley	1
Solar Turbines International P.O. Box 80966 San Diego, California 92138 Attention: G.W. Hosang	1

	No. of Copies
Southwest Research Institute P.O. Drawer 28510 San Antonio, Texas 78228	1
Materials Sciences & Engineering Laboratory Stanford Research Institute Menlo Park, California 84025 Attention: Dr. Cubiciotti	1
Teledyne CAE 1330 Laskey Road Toledo, Ohio 43601 Attention: Hugh Gaylord	1
Union Carbide Corporation Parma Technical Center P.O. Box 6116 Cleveland, Ohio 44101	1
Materials Sciences Laboratory United Aircraft Corporation East Hartford, Connecticut 06101 Attention: Dr. J.J. Brennan	1
Astronuclear Laboratory Westinghouse Electric Corporation Box 10864 Pittsburgh, Pennsylvania 15236	1
Westinghouse Research Laboratories Beulah Road Churchill Borough Pittsburgh, Pennsylvania 15235 Attention: Dr. R. Bratton	1